Turkish J. Eng. Env. Sci.
31 (2007) , 89 – 118.

Experimental Investigation of the Mechanical Behavior of Solid and Tubular Wood Species under Torsional Loading

Ezgi GÜNAY
Gazi University, Department of Mechanical Engineering, 06570, Ankara-TURKEY
e-mail: egunay@gazi.edu.tr
Yusuf ORÇAN
Middle East Technical University, Department of Engineering Sciences, 06531, Ankara-TURKEY

Received 27.09.2006

Abstract

Torsion experiments are performed in order to examine the mechanical behavior of Turkish beech, pine, hornbeam, and chestnut wood specimens. Solid and tubular bars of different geometries are tested under torsional loading. The results are compared for different species and geometries of wood specimens. The shear stress-strain curves are obtained in order to show their characteristic behavior in detail. The data obtained from torsional loading experiments are used to estimate the modulus of rigidity of different wood specimens. The factors affecting the slopes of the characteristic shear stress-strain curves of different wood species under forward/backward and cyclic loading are discussed. Stress relaxation tests are performed on both pine and beech for torsional loading.

Key words: Wood, Torsion tests, Shear modulus, Solid and tubular bars, Cyclic loading, Size effect.

Introduction

Interest in the determination of mechanical properties of wood under the action of different types of loading has never ceased. Wood fibers from a micromechanical point of view and wood materials at macro level have been examined under different assumptions. Mack (1940) studied small-scale, circular specimens under torsion in order to obtain the shear strength of wood. Mack (1979) introduced the Australian standard test methods among the other common test methods (BSI-The British Method, 1957; ASTM method of testing, 1972) for small clear specimens of timber. Pagano and Kim (1988) considered graphite-fiber carbon-matrix composite material tube specimens subjected to torsional loading and studied the interlaminate shear stresses. Woodward and Minor (1988) examined Douglas fir timbers for the determination and comparison of the failure formulas for 6 different grain angles. Tsai and Daniel (1990) studied prismatic composite specimens for the determination of the 3 principle shear moduli: G_{12}, G_{23} and G_{13}. The chosen graphite/epoxy and silicon carbide/glass ceramic type specimens were tested under torsional loading. They obtained a closed form relationship between the angle of twist and the applied torque. Tsai et al. (1990) included the shear properties of the composite specimen for each layer. The chosen composite material was unidirectional composite graphite/epoxy, and 3 principal shear modulus values,G_{12}, G_{23} and G_{13}, were used in their expressions. Hayashi et al. (1993) studied the response of wood specimens to tensile loading and obtained viscoelastic compliance terms for 12% equilibrium moisture content. It was observed that the time-dependent strain reduced the ultimate strength by 58%. The compliances were represented by time power functions. Hayashi et al. (1993) studied wood for the determination of 4 compliance terms under a tensile test. Govic et al. (1994) explained the main methods for tensile and compression tests on Okoume poplar, maritime pine, plywood, and

particle board. Ifju (1994) introduced a shear gauge for reliable shear modulus measurements. Park and Balatinecz (1997) investigated the mechanical properties of wood-fiber/toughened polypropylene composites. Wood-fiber thermoplastic composites were prepared with isotactic polypropylene. They showed that the fibers of wood increased the stiffness and the percentage elongation at break and decreased the impact strength. Rezai and Warner (1997) investigated the water absorbance of wood fibers. Dinus and Welt (1997) gave a review of fiber properties with the help of biological methods. Liu (1997) performed a viscoelastic 2-dimensional finite element analysis of vacuum forming of wood fiber filled with isotactic polypropylene. The analysis showed that the viscoelastic effect of the polymer should not be neglected in the modeling of a vacuum-forming problem. Liu and Ross (1998) investigated the mechanical property variations in wood with grain slope.

Experimental studies using nondestructive evaluation (NDE) and nondestructive test (NDT) methods showed that the properties of wood are affected by the growth rate, internal decay, defect distribution, and density variation separately. The ultrasonic stress wave method for the detection of deflection was proposed by Mal et al. (1988) and Beall (1987) for nondestructive testing of wood. Bodig (2001) explained the pseudo-NDE techniques such as deflection method, electrical properties, gamma radiation, penetrating radar method, and X-ray method.

Rammer et al. (1996) described experimental studies for the determination of shear strength, size effect, and fracture of Engelmann spruce, Douglas fir, and southernwood type beams. They pointed out that the shear strength of wood varies with size, shear surface area, and volumetric change. Shear strength of wood (Forest Products Laboratory, 1999) was based on the shear block test (ASTM, 1978). March et al. (1942) introduced a method called the plate twist test (ASTM, 1976) to measure the shear modulus of wood. This test did not consider the effect of grain slope; nevertheless, the test findings were compared with shear text fixture and analytical equations by Liu (2000). Here, the used wood specimens were Sitka spruce (*Picea sitchensis*) ($E_1 = 11.8$ MPa, $E_2 = 2.216$ MPa, $G_{12} = 910$ MPa, $\nu_{12} = 0.37$). The shear strain γ_s values were measured with 45° strain rosette and shear gauge (see Appendix). Liu (2000) studied the effects of shear coupling on the shear properties of wood. Liu et al. (1999) presented a shear test fixture using the Iosipescu specimen. Yoshihara et al. (2001) studied rectangular wood specimens to determine the shear stress-strain equations. The research included the experimental results obtained by the Iosipescu shear test and torsion test with their comparisons. The assumed approximated equation for shear modulus by Lekhnitskii (1963) and Yoshihara et al. (1993) (see Appendix) was used and the numerical results were discussed. The specimens used were Sitka spruce (*Picea sitchensis* Sarr.) and Shioji (Japanese ash, *Faxinus spaethiana* Lingelsh).

Yamasaki and Sasaki (2000a, 2000b) studied the failure behavior of Japanese beech wood under combined axial force and torque in order to check the failure behavior of wood for grain angles $-90° \langle \theta \langle 90°$. Zidi (2000) studied the finite torsion problem of anisotropic solid and tubular bars numerically.

Örs et al. (2001) studied the layered wood shell structures under shear, tensile, and bending tests. The timber used was poplar (*Populus xeureamericana* I 45/51). The results obtained show that the mechanical properties of plywood can be improved by changing the pressure, press time, and thickness of veneer parameters during the preparation of the layers. Groom et al. (2002) determined the Young's modulus and ultimate tensile stress of pine single wood fiber within the ranges 6.55-27.5 GPa and 410-1422 MPa for different tree heights and juvenilities.

Bucur and Rasolofosaon (1998) used ultrasonic wave propagation techniques in order to explain the anisotropic and nonlinear elastic behavior of wood and rock. Bucur (2003) assumed that wood has a triclinic symmetry and obtained the elastic material constants matrix $[C_{ij}]$ using ultrasonic methods. In a review article by Bucur (2003), the main measurement techniques on material properties of wood were discussed. They were grouped as ionizing radiation, microwaves, ultrasonic, nuclear magnetic resonance, and X-ray methods. In a related study, Bucur et al. (2002) presented the related equations for the analytical propagation of ultrasonic waves. Winandy (1994), and Winandy and Rowell (2005) explained the micro- and macrostructural concepts of wood in a general view.

Gunay and Sonmez (2003) investigated experimentally the mechanical behavior of Turkish beech, pine and oak wood using solid round specimens subjected to torsional and tensile loadings.

Nafa and Araar (2003) presented some applied data concerning the torsional behavior of glued-laminated wood beams under several loading pro-

grams. They have shown the failure characteristics of the studied beams in monotonous torsion and the influence of the loading amplitude in cyclic torsion.

Chen et al. (2006) presented the results of a series of experiments on hardwood (red lauan) and softwood (Sitka spruce) test pieces under static and cyclic torsional loading. It was noted that most research has focused on wood laminates and for applications such as wind turbine blades, since wood has several advantages over other materials for blade construction. They have shown that the strength of both hardwood and softwood decreased as the grain orientation of the sample to the axis of twist increased from 0° to 90° with a corresponding decrease in elastic modulus under static torsional loading. The authors noted that hardwood shows a small decrease in stiffness with each loading cycle prior to failure, whereas the stiffness of the softwood only changes slightly before failure. Results of the hysteresis loop for a hardwood show that before cracking occurs the hysteresis loop area and maximum shear stress at each cycle decrease with an increase in cyclic loading. This is a relaxation behavior that has been reported by Bodig and Jayne (1982) and Kollmann and Coté (1968).

The aim of this article is to examine the mechanical response of Turkish pine, beech, hornbeam, and chestnut under torsional loading for solid and tubular type specimens with different radial dimensions. With the help of a series of experiments, the general behavior characteristics of the stress-strain response of wood specimens are obtained comparatively.

Experimental

Solid and tubular test specimens

The geometries of solid and tubular specimens in torsion experiments were chosen from 4 different outer diameters:$d_1 = 12.50$ mm, $d_2 = 12.0$ mm, $d_3 = 10.00$ mm and $d_4 = 7.0$ mm. The tubular specimens were produced using a drilling process and the exact inner diameters were measured and found to be 6.0, 6.3, 6.4, 6.5, 6.6, 6.8, 7.6 and 9.2 mm, while the outer diameters were chosen the same as the outer diameters of the solid specimens mentioned above. A fixed gauge length $L_g = 90$ mm was used in the torsion experiments, whereas the total length L of the specimen was taken as 150 mm. A and H are the dimensions of the grip section (Figure 1). The value of H was taken as 25, 21 and 13.5 mm and the size A was taken as 30 mm.

Experimental Method

Torsion tests were performed at a room temperature of 15-17 °C in winter. The average moisture content of the test specimens was measured using a Delmhorst Instrument BD-10 moisture meter for

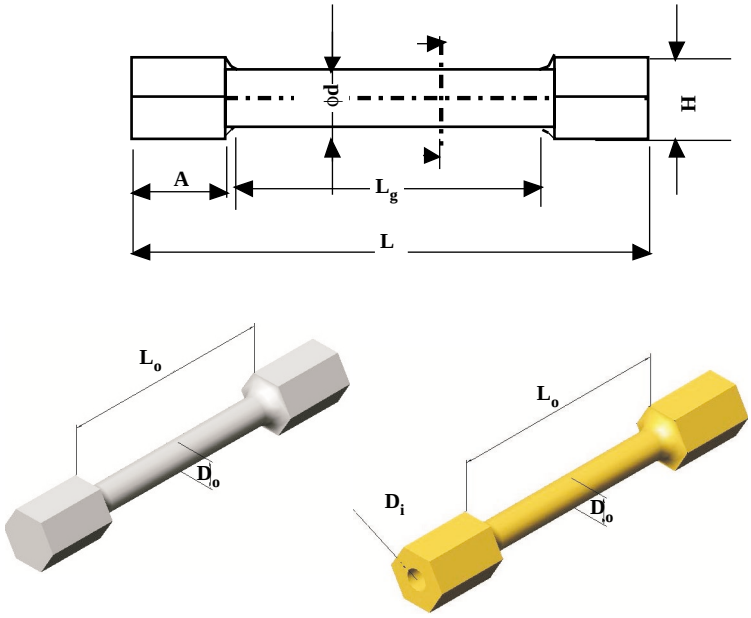

Figure 1. Geometries of solid and tubular specimens used in torsion tests.

wood and found to be 6%. The longitudinal axes of the wood specimens were chosen parallel to the grain directions. However, each wood specimen had different grain angles, θ, which vary between 0° and +35°.

The main groups of the research are as follows:

- Torsion tests on beech, pine, hornbeam and chestnut specimens (Figure 1) that have solid circular cross sections with 3 different radii,
- Torsion tests on pine, chestnut and steel specimens that have tubular circular cross sections having the same outer but different inner radii,
- Cyclic torsion tests on solid circular wood specimens having the same outer radii (Figure 3).

Torsion tests were performed starting from zero torque value until the failure torque values were reached at constant strain rates in different phases of the loading procedure. The tests were performed at slow strain rates until the specimen yielded. After that, the motor speed was increased until the failure stage of the test was reached. The torsion testing machine SM21 (TecQuipment, 1982) has a digital counter, each data-counter increment of which corresponds to a 0.3° angle of twist. Each value of the angle of twist ϕ was transformed to γ_{12}^m, the maximum shear strain at the cross section for both solid and tubular bars. Indices 1, 2, and 3 represent the principal directions of the corresponding orthogonal coordinate system, which is attached at an edge of the cross section (Figures 2 and 3). Axes 2 and 3 lie in the cross section whereas axis 1 is parallel to the longitudinal twist axis. Wood is assumed to be an transversely isotropic composite material. The independent elastic constants for orthotropic and for the special case of the transversely isotropic materials are given in the Appendix.

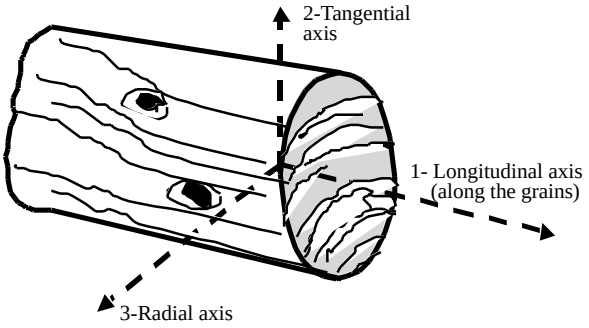

Figure 2. General specification of orthotropic material with the principal directions.

The stress-strain relationships in torsional loading can be written as $\gamma_{12}^m = \tau_{12}^m/G_{12} = r_o\,\phi^m/L_g$ and $\tau_{12}^m = T\,r_o/J = 2\,T/\pi\,r_o^3$. Here, r_o is the outer radius, τ_{12}^m is the maximum shear stress developing at each cross section, G_{12} is the shear modulus, T is the instantaneously applied torque by the torque-machine, and J is the polar moment of inertia of the cross section of solid or tubular bars.

Results and Discussion

In Tables 1 and 2, the available elastic mechanical constants of typical wood specimens from the literature are listed. As can be seen, there are still unknown material specifications for some wood species. In Tables 3-6, the shear modulus values of pine, beech, chestnut, and hornbeam wood obtained from the present study are listed both for the solid and tubular circular cross-sectional bars. Statistical values showing the central tendency and the spread of data for all experimental results are listed in Table 7 comparatively.

Static torsion tests without unloading

Figure 4 shows the stress-strain graphs for different r/L parametric ratios of pine and beech solid test specimens. Note that shear stresses take negative values when the test specimens are subjected to backward directional torsional loading. The stress increases sharply in thin bars with $r/L = 0.07$ compared to the thick ones with $r/L = 0.13$ at the same angle of twist in the range of $0.0075 - 0.015$. It is noted from Figure 4 that thin solid bars yield at $\gamma_{12} = 0.016$ and $\tau_{12} = 46$ MPa, while the thick solid specimens continue to deform at a comparatively small rate up to $\gamma_{12} = 0.05$.

Figures 5 and 6 show that tubular pine wood bars break at a smaller angle of twist compared to tubular hornbeam bars, while the shear stress levels at cracking are slightly higher. It is noted that the stress-strain curves are parallel to each other and their slopes are approximately the same. Sometimes, due to undetected production damage, specimens exhibit stress-strain curves with extraordinary slopes. Figure 6 displays the stress-strain behavior of tubular hornbeam. The 2 tubular hornbeam bars failed at relatively large strain values compared to the other 6 species (Figure 1).

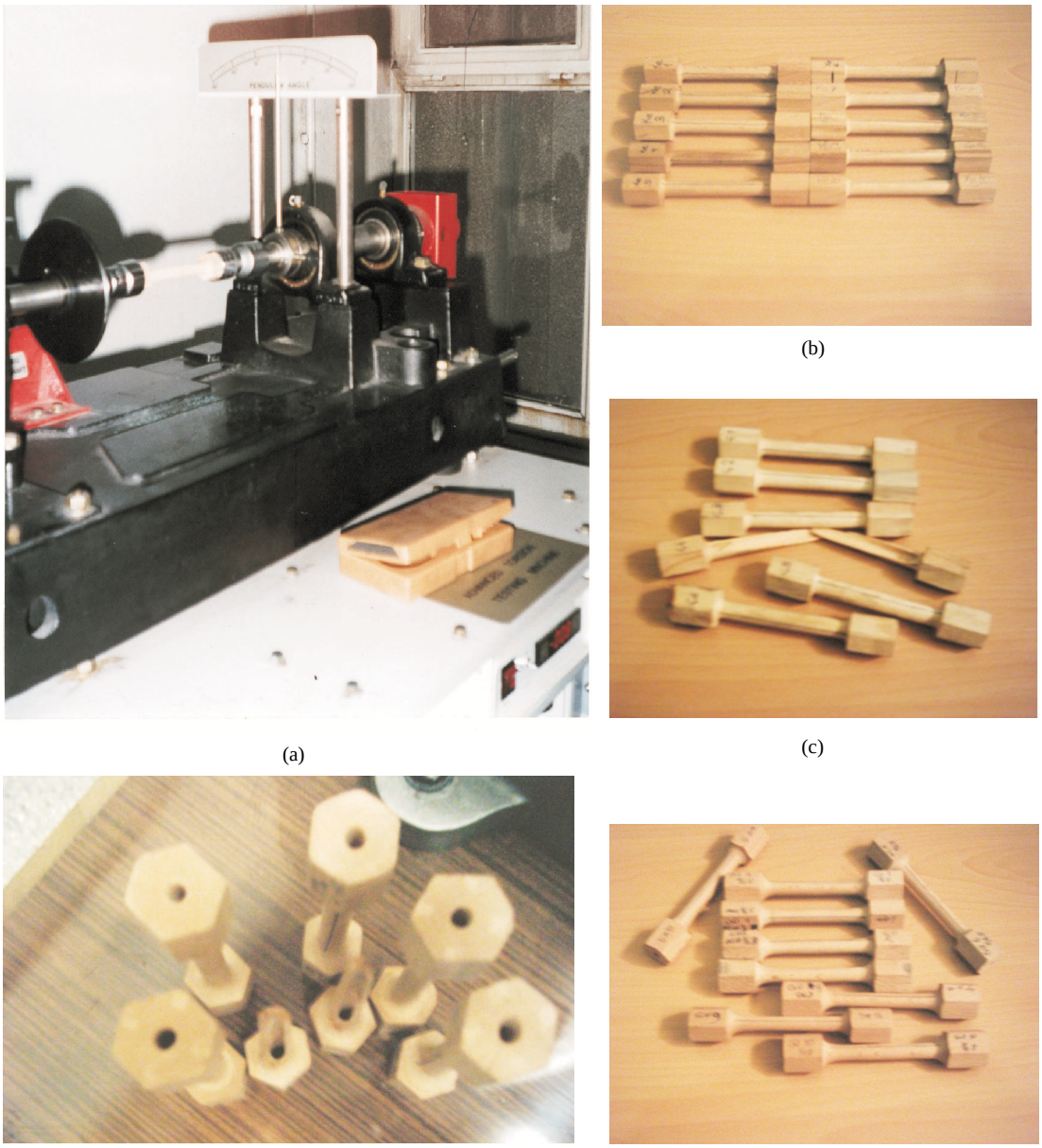

Figure 3. (a) TQ-SM21 torsion test fixture and (b) chestnut, (c) pine, (d) beech, (e) hornbeam tubular and solid wood test species.

Table 1. Mechanical properties of different types of wood (Hibbeler, 1991; Chandrupatla, 1997).

Wood Species	E_1 GPa	$\frac{E_1}{E_2}$	ν_{13}	G MPa	$\frac{E_1}{G_{32}}$	σ_T (Elastic Tensile Strength) MPa	σ_C (Elastic Comp. Strength) MPa	σ_{uT} (Ultimate Tensile Strength) MPa	σ_{uC} (Ultimate Comp. Strength) MPa	τ_{13} MPa
Balsa wood	0.83	20.0	0.30	-	29.0	-	-	-	-	-
Pine wood	9.81	23.8	0.24	-	13.3	-	-	-	-	-
Plywood	11.7	2.00	0.07	-	17.1	-	-	-	-	-
Douglas fir, green	11.0	-	-	-	-	33	23	-	27	6.2
Douglas fir	23.5-24.5	-	-	-	-	-	-	853 - 912	-	-
Douglas fir, air dry	13.00-13.01	-	2.10	-	-	56	44	-	26-51	6.2-7.6
Red oak, green	10.00	-	-	-	-	30	18	-	24	8.3
Red oak, air dry	12.00	-	-	-	-	58	32	-	48	12.4
White spruce	9.65	-	0.31	-	-	-	-	2.5	36	6.7
Loblolly pine latewood	6.55 - 27.5	-	-	-	-	-	-	410 -1422	-	-

Table 2. Typical elastic constants of some wood material (Chandrupatla, 1997).

Wood Types	E_1 GPa	E_2 GPa	E_3 GPa	G_{21} GPa	G_{32} GPa	G_{31} GPa	ν_{21}	ν_{32}	ν_{31}
Douglas fir	14.8	0.6	1.0	0.7	0.1	0.8	0.017	0.432	0.0216
Spruce Hexagonal Model	0.0143	1.120	0.556	0.605	0.035	0.594	0.049	0.11	0.022
Spruce measurement	6.0-25.	0.7-1.2	0.4-0.9	0.6-.07	0.02-0.7	0.5-0.6	0.02-0.05	0.2-0.35	0.01-0.025

Table 3. Shear modulus values of circular cross-sectional pine wood specimens under torsional loading.

Test No	Wood specimen and loading types: Forward loading - F, Backward loading - B, Solid specimen - S, Tubular specimen - T	Radius (mm) r_i : inner, r_o : outer	G_{12} (GPa)
1	White Pine- T - F	r_i=4.6, r_o =6.0	3.01
2	White Pine- T - B	r_i=4.6, r_o =6.0	9.03
3	White Pine- T - F	r_i=3.4, r_o =6.0	7.34
4	White Pine- T - F	r_i=3.2, r_o =6.0	3.77
5	White Pine- T - B	r_i=4.6, r_o =6.0	9.03
6	White Pine- T - B	r_i=4.6, r_o =6.0	11.4
7	Pine -T - F	r_i=3.2, r_o =6.0	5.51
8	Pine - T - F	r_i=3.2, r_o =6.0	5.88
9	Pine -T - F	r_i=4.6, r_o =6.0	7.48
10	Pine -T - F	r_i=4.6, r_o =6.0	2.84
11	Pine -T - F	r_i=4.6, r_o =6.0	8.26
12	Pine -T - F	r_i=4.5, r_o =6.0	7.88
13	Pine - T - F	r_i=4.6, r_o =6.0	6.69
14	Pine -T - F	r_i=4.5, r_o =6.0	1.30
15	Pine -T - F	r_i=4.6, r_o =6.0	2.19
16	Pine - T -F	r_i=3.0, r_o =6.0	2.18
17	Pine - T -F	r_i=3.0, r_o =6.0	3.53
18	Pine - T -F	r_i=3.0, r_o =6.0	3.45
19	Pine -S -F	r_o =6.25	1.44
20	Pine -S -B	r_o =6.25	2.09
21	Pine -S -B	r_o =3.5	2.19
22	Pine -S -B	r_o =5.00	1.57
23	Pine -S -B	r_o =5.00	5.98
24	Pine -S -B	r_o =5.00	2.82
25	Pine -S -B	r_o =6.00	5.24
26	Pine -S -F	r_o =6.00	4.25
27	Pine -S -F	r_o =6.00	1.11
28	Pine - S -F	r_o =6.00	1.92
29	Pine -T - B/F(avg-forward-backward)	r_i=4.5, r_o =6.1	3.25
30a	Pine -S -F - 1st cycle	r_o =10.0	0.18
30b	Pine -S -B - 2nd cycle	r_o =10.0	0.35
30c	Pine -S -F - 3rd cycle	r_o =10.0	0.40
30d	Pine -S -B - 4 th cycle	r_o =10.0	0.33
30e	Pine -S -F - 5 th cycle	r_o =10.0	0.35

Table 4. Shear modulus values of circular cross-sectional hornbeam wood specimens under torsional loading.

Test No	Wood specimen and loading types: Forward loading - F Backward loading - B Solid specimen - S Tubular specimen - T	Radius (mm) r_i : inner r_o : outer	G_{12} (GPa)
1	Hornbeam -T -F	r_i=3.0, r_o =5.8	1.36
2	Hornbeam -T -F	r_i=3.2, r_o =6.0	2.62
3	Hornbeam -T -F	r_i=3.3, r_o =6.0	7.72
4	Hornbeam -T -F	r_i=3.2, r_o =6.0	7.40
5	Hornbeam -T -F	r_i=3.2, r_o =6.0	7.50
6	Hornbeam -T -F	r_i=3.2, r_o =6.0	2.02
7	Hornbeam -T -F	r_i=3.2, r_o =5.9	2.90
8	Hornbeam -T -B	r_i=3.15, r_o =6.0	7.31
9	Hornbeam -T -F	r_i=3.3, r_o =5.7	1.45
10	Hornbeam -T -F	r_i=3.8, r_o =6.0	2.41
11	Hornbeam -T -F	r_i=3.2, r_o =6.0	3.12
12	Hornbeam -T - F	r_i=3.2, r_o =6.0	2.76
13	Hornbeam -T - F	r_i=3.0, r_o = 6.0	3.78
14	Hornbeam -T - F	r_i=3.3, r_o = 6.0	1.30
15	Hornbeam -S -F	r_o =6.0	2.53
16	Hornbeam -S -F	r_o =6.0	4.39
17	Hornbeam -S - F	r_o =6.1	1.34
18	Hornbeam -S - F	r_o =6.1	3.64
19	Hornbeam -S - F	r_o =6.1	3.80
20	Hornbeam -S - F	r_o =6.0	3.06
21	Hornbeam -S - B	r_o =6.1	0.83
22	Hornbeam -T -B/F(avg-forward-backward)	r_i=3.25, r_o =6.0	3.40
23	Chestnut -T -F	r_i=3.25, r_o = 6.0	7.33
24	Chestnut -T -F	r_i=3.30, r_o = 6.0	7.18
25	Chestnut -T -F	r_i=3.25, r_o = 6.0	1.48

Table 5. Shear modulus values of circular cross-sectional chestnut wood specimens under torsional loading.

Test No	Wood specimen and loading types: Forward loading -F Backward loading - B Solid specimen - S Tubular specimen - T	Radius (mm) r_i : inner r_o : outer	G_{12} (GPa)
1	Chestnut -T -F	r_i=3.25, r_o = 6.0	7.33
2	Chestnut -T -F	r_i=3.30, r_o = 6.0	7.18
3	Chestnut -T -F	r_i=3.25, r_o = 6.0	1.48
4	Chestnut -T -F	r_i=3.10, r_o = 5.9	3.55
5	Chestnut -T -F	r_i=3.30, r_o = 6.0	5.97
6	Chestnut -T -F	r_i=3.00, r_o = 6.0	1.82
7	Chestnut -T -F	r_i=3.25, r_o = 6.0	6.62
8	Chestnut -T -F	r_i=3.00, r_o = 6.0	6.12
9	Chestnut -T -F	r_i=3.20, r_o = 5.9	5.57
10	Chestnut -T -F	r_i=3.10, r_o = 6.0	7.53
11	Chestnut -T -F	r_i=3.0, r_o =6.00	7.75
12	Chestnut -T -F	r_i=3.0, r_o =6.0	5.22
13	Chestnut -T -F	r_i=3.25, r_o =6.0	0.65
14	Chestnut -T -B	r_i=3.0, r_o =6.0	1.98
15	Chestnut -T -B	r_i=3.15, r_o =6.0	7.01
16	Chestnut -T -B	r_i=3.15, r_o =6.0	0.98
17	Chestnut -T -F	r_i=3.0, r_o =6.0	3.21
18	Chestnut -T -F	r_i=3.0, r_o =6.0	3.61
19	Chestnut -S -F	r_o =6.0	2.07
20	Chestnut -S -B	r_o =6.01	0.17
21	Chestnut -S -F	r_o =6.01	0.40

Table 6. Shear modulus values of circular cross-sectional beech wood specimens under torsional loading.

Test No	Wood specimen and loading types: Forward loading -F Backward loading - B Solid specimen - S Tubular specimen - T	Radius (mm) r_i : inner r_o : outer	G_{12} (GPa)
22	Beech -S -B	r_o =6.25	0.93
23	Beech -S -B	r_o =6.25	2.15
24	Beech -S -B	r_o =5.00	2.80
25	Beech -S -B	r_o =6.25	1.72
26	Beech -S -B	r_o =3.50	5.60
27	Beech -S -B	r_o =3.50	7.66
28	Beech -S -B	r_o =3.50	1.00
29	Beech -S -B	r_o =5.00	0.53
30a	Beech -S - 1st cycle	r_o =6.25	8.62
30b	Beech -S - 6th cycle	r_o =6.25	9.48
30c	Beech -S - 9 th cycle	r_o =6.25	10.8
31a	Beech -S - 1st cycle	r_o =6.25	6.48
31b	Beech -S - 7th cycle	r_o =6.25	10.14
31c	Beech -S - 7th cycle	r_o =6.25	5.75
31d	Beech -S - 9th cycle	r_o =6.25	9.06
32	Beech -T - B/F(avg-forward-backward)	r_o =6.25	7.42
33a	Beech -S - 2nd cycle	r_o =6.25	4.73
33b	Beech -S - 4th cycle	r_o =6.25	6.32
33c	Beech -S - 5th cycle	r_o =6.25	9.48

Table 7. Statistical values of shear modulus for Turkish wood species.

Type of wood (number of species)	Average Shear Modulus G_{12} (GPa)	Standard Deviation (GPa)	Coefficient of variation c.v. (%)
Pine(solid+tube) (24)	3.72	3.64	97.67
Pine(solid+tube)-without cyclic load (22)	3.90	-	95.24
White pine (6)	7.26	5.77	79.44
Tubular pine (13)	4.65	3.87	83.21
Solid pine (11)	2.63	2.69	102.54
Solid pine-without cyclic load (10)	2.86	2.85	99.44
Hornbeam(solid+tube) (22)	3.48	3.37	96.76
Hornbeam(solid+tube) without cyclic load (21)	3.48	3.37	96.59
Tubular hornbeam (14)	3.83	3.46	90.41
Solid hornbeam (7)	2.80	1.66	59.25
Chestnut(solid+tube) (21)	4.11	4.32	105.10
Solid chestnut (3)	0.88	1.04	117.84
Tube chestnut (18)	4.64	4.63	99.66
Pine(solid+tube)- forward load (15)	2.69	3.75	119.67
Tubular pine- forward load (12)	4.77	3.90	81.89
Solid pine- backward load (6)	3.32	2.85	85.98
Tubular hornbeam- forward load (13)	3.56	2.99	83.75
Tubular hornbeam- backward load (1)	7.31	-	-
Solid hornbeam- forward load (6)	3.13	1.74	55.81
Solid hornbeam- forward load (1)	0.83	-	-
Chestnut(solid+tube) –forward load (17)	4.48	4.44	99.20
Tubular chestnut–backward load (3)	3.32	3.23	97.24
Solid chestnut–backward load (1)	0.17	-	-
Tubular chestnut–forward load (15)	4.91	4.70	95.76
Solid chestnut–forward load (2)	1.24	2.44	197.84
Beech (solid+tube) –forward load (12)	4.51	5.61	124.42
Solid beech - backward direction and without cyclic load (8)	1.87	3.22	140.65

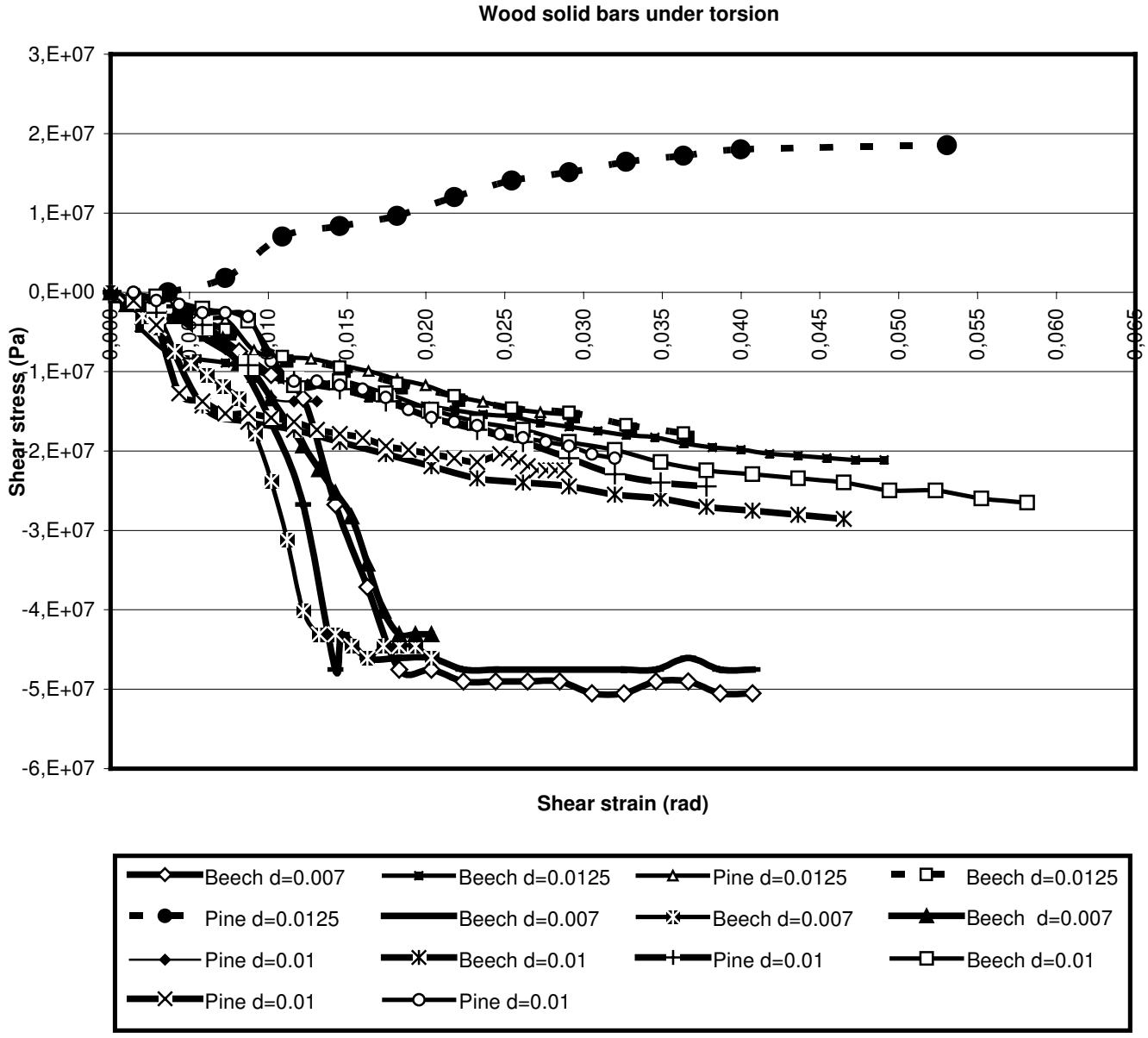

Figure 4. Curves for Turkish pine and beech wood solid specimens under 1 forward and 13 backward torsional loading for d_o(m).

Figures 7-9 represent the tubular hornbeam, pine, and chestnut wood specimens under backward and forward torsional loading. These series of experiments have been carried out with variable inner radial dimensions of specimens. t/r_o ratios of these specimens lie in the ranges of $0.5 \langle (t/r_o)_{hornbeam} \langle 2.6$, $0.23 \langle (t/r_o)_{pine} \langle 0.25$, and $0.45 \langle (t/r_o)_{chestnut} \langle 0.5$. In Figures 7-9, when we compare the shear stress values at the same shear strain $\gamma = 0.015$ (rad), it is seen that the average torsional shear stresses of the samples satisfy the inequality $\tau_{pine} \langle \tau_{chestnut} \langle \tau_{hornbeam}$. The minimum torsional shear stress at the same shear strain $\gamma = 0.015\,(rad)$ occurs for pine tubular specimens that have relatively small wall thicknesses.

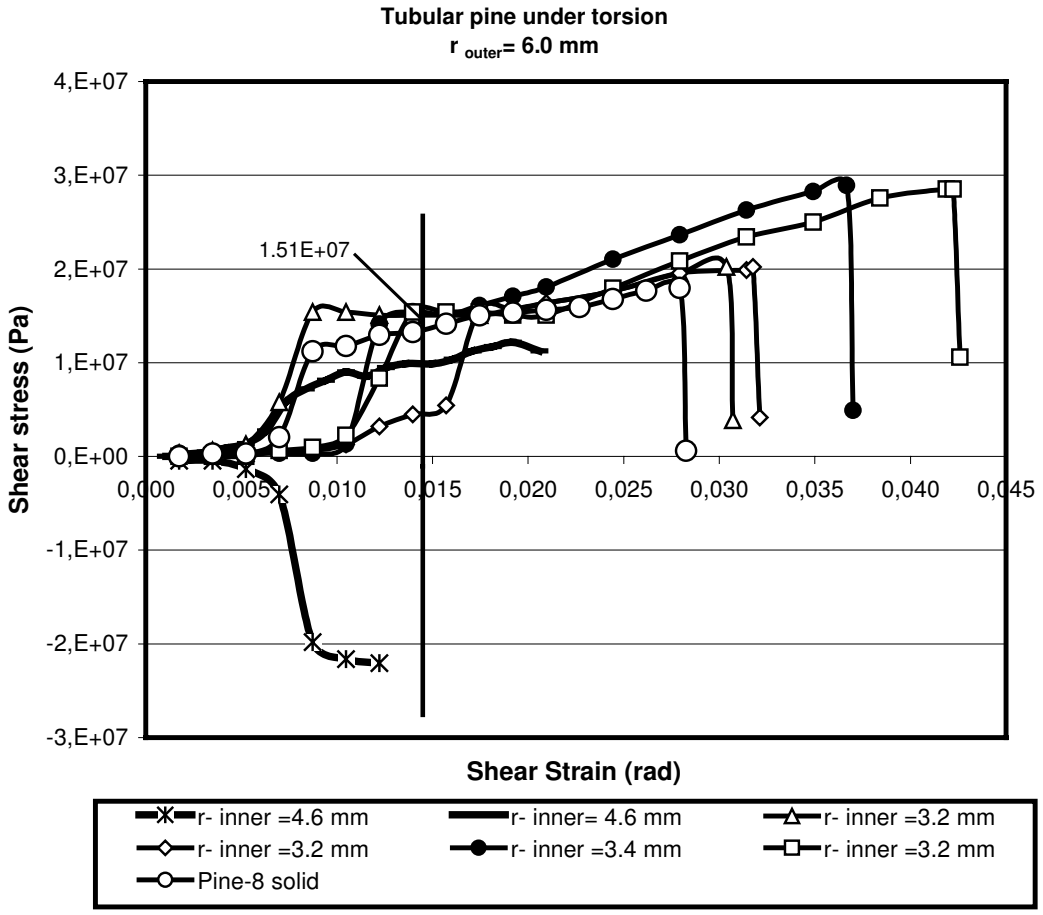

Figure 5. Curves for 7 tubular and 1 solid pine wood specimens under forward/backward torsional loading.

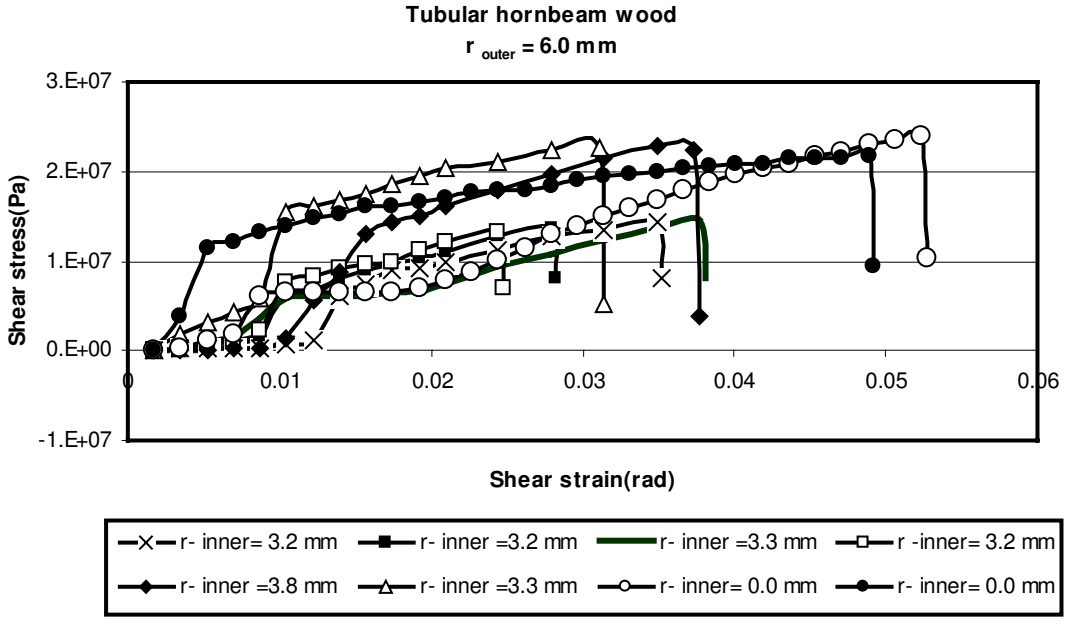

Figure 6. Curves for tubular hornbeam wood specimens under forward torsional loading.

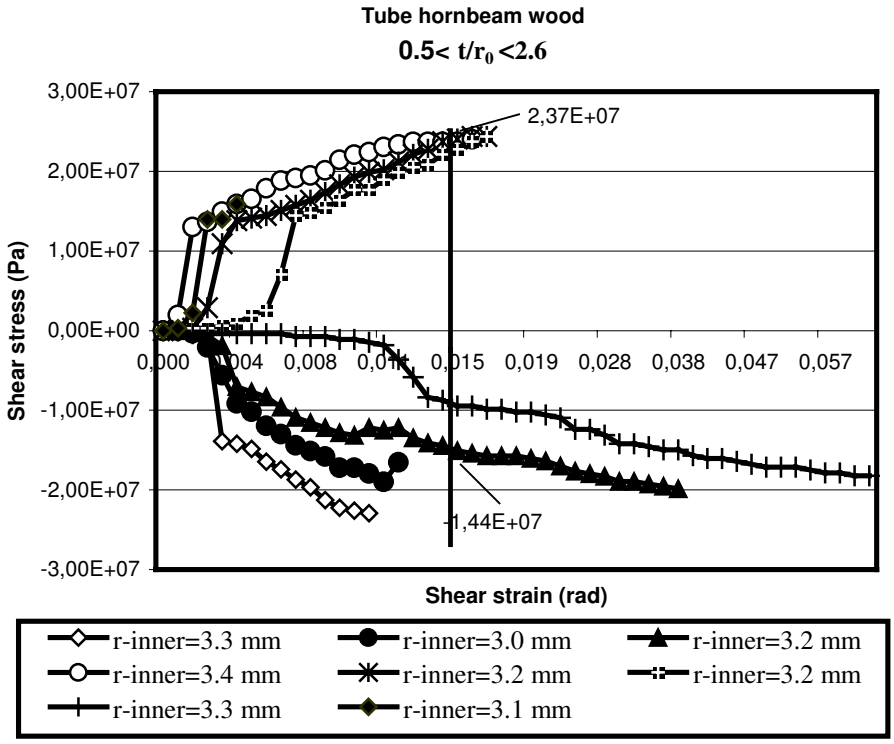

Figure 7. Curves for tubular hornbeam wood specimens under forward and backward torsional loading for $r_o = 6\,mm$.

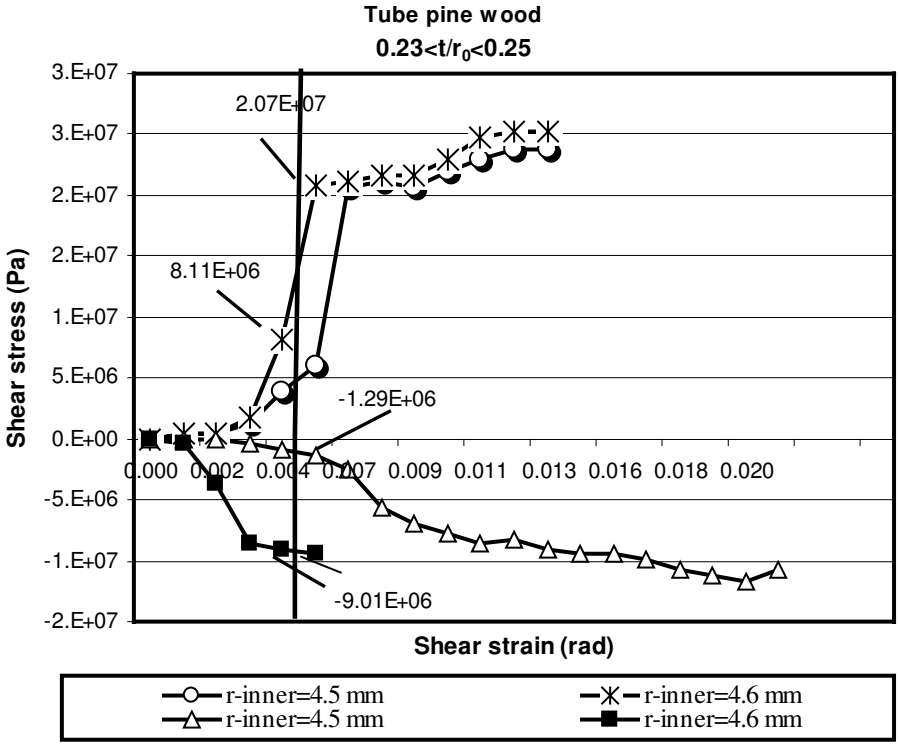

Figure 8. Curves for tubular pine wood specimens under forward and backward torsional loading for $r_o = 6\,mm$.

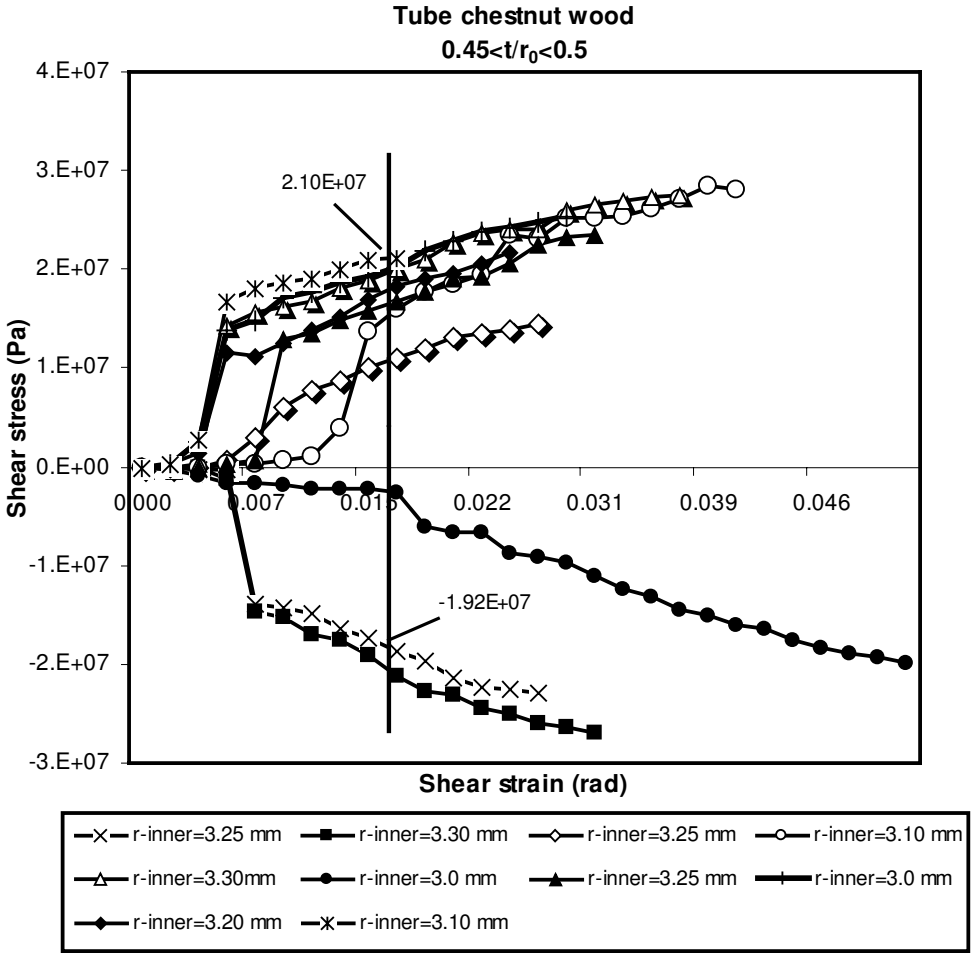

Figure 9. Curves for tubular chestnut wood specimens under forward and backward torsional loading for.

The effect of specimen size and load application direction on the mechanical response is shown in Figure 10 for chestnut tubular wood. Tubular chestnut specimens with $0.475 \langle (t/r_o)_{chestnut} \langle 0.5$ show similar shear stress values at $\gamma = 0.015\,(rad)$(Figures 9 and 10). The grain angles affect the values of maximum torsional shear stress ($\tau_{\max}$) in the consideration of the effect of forward and backward loading. If the sample has a grain orientation $\theta = 0^\circ$ to the twist axis, it is shown that forward and backward directional loading gives symmetrical $\tau - \gamma$ curves. Otherwise, if the samples have grain orientations greater than $\theta = 0^\circ$, the forward directional shear stress is higher than the backward directional one. This is attributed to the fact that for forward torsional loading when $\theta > 0^o$, in addition to the shear stress, tensile normal stress occurs perpendicular to the failure surfaces that lie along the grain orientations. On the other hand, for backward torsional loading the normal stress component is compressive, which increases the failure strength of the test specimens. Tubular white pine (Figures 11 and 12) and pine (Figures 5, 8, and 10) can be compared with each other by considering the stresses at a selected fixed value of the angle of twist. Taking $\gamma = 0.015\,(rad)$, Figures 5, 8, and 10-12, respectively, give the torsional shear stresses for forward (positive) and backward (negative) loadings as $\tau = 15.1$ MPa, $\tau = 20.7$ MPa, $\tau = -9.01$ MPa, $\tau = -1.29$ MPa, $\tau = 20.4$ MPa, $\tau = -18.5$ MPa, $\tau = 9.46$ MPa, and $\tau = -21.6$ MPa. Additionally, white pine has a higher stress carrying capacity compared to pine and when the shear moduli are compared it is found that $(G_{w-pine})_{avg} = 7.26 \rangle (G_{pine})_{avg} = 3.72$ (see Tables 3-7).

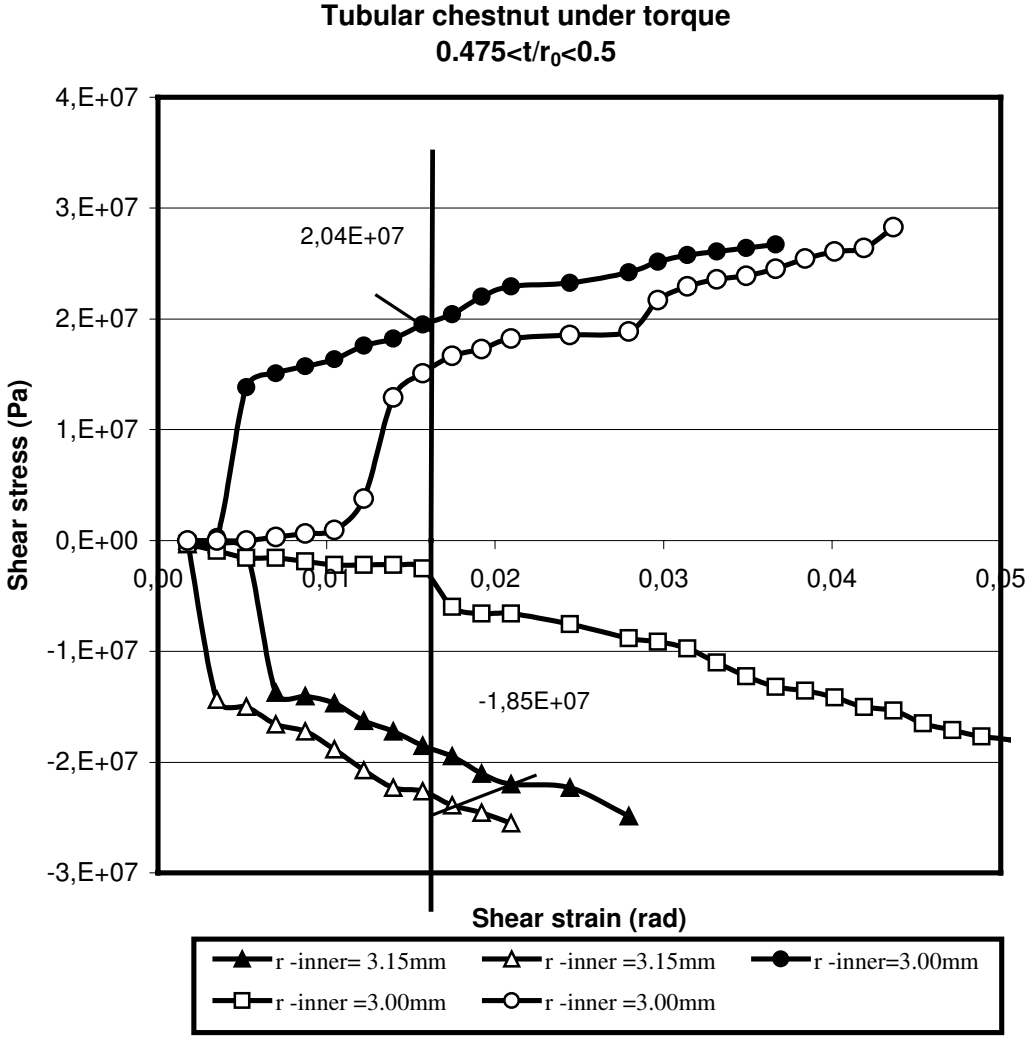

Figure 10. Curves for tubular chestnut wood specimens under forward/backward loading for $r_o = 6\,mm$.

In order to compare the behavior of metals with wood material, torsion tests of tubular Steel 1010 were performed and the stress-strain distribution obtained is illustrated in Figure 13. It can be noted here that wood shows a slight parabolic curve in its linear range, while metals exhibit a perfectly linear response in the elastic range.

Figures 14-17 show the effect of different r/L and t/r_oratios on the stress-strain relation for different wood species and the load application directions. The maximum shear strain values of all wood specimens were less than 0.06 rad. From the torsion tests the average shear modulus values for pine and beech were $G_{12\,avg}^{pine} \approx 3.72\,GPa$ and $G_{12\,avg}^{beech} \approx 4.51\ GPa$. Xavier et al. (2004), Pereira (2004), and Forest Products Laboratory (1999) gave the shear modulus values of maritime pine as $G_{23} = 0.176$ (GPa), $G_{13} = 1.096$ (GPa), and $G_{12} = 1.109$ (GPa). They reported that beech wood reaches the approximate yield stress value $(\tau_{12})_Y^{beech} = 53.21$ (MPa) while pine reaches $(\tau_{12})_Y^{pine} = 42.0$ (MPa) under torsional loading. The measured ultimate average shear stresses using the Iosipescu tests were $\tau_{12}^{ult} = 16.9$ MPa, $\tau_{13}^{ult} = 18.1$ MPa, and $\tau_{23}^{ult} = 4.35$ MPa.

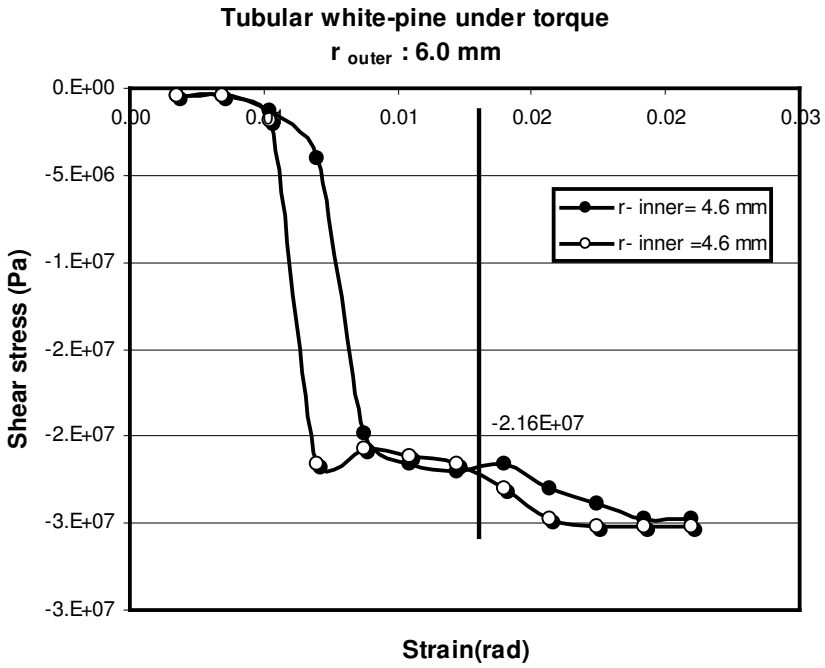

Figure 11. Curves for tubular white-pine wood specimens under backward loading for $r_o = 6\,mm$.

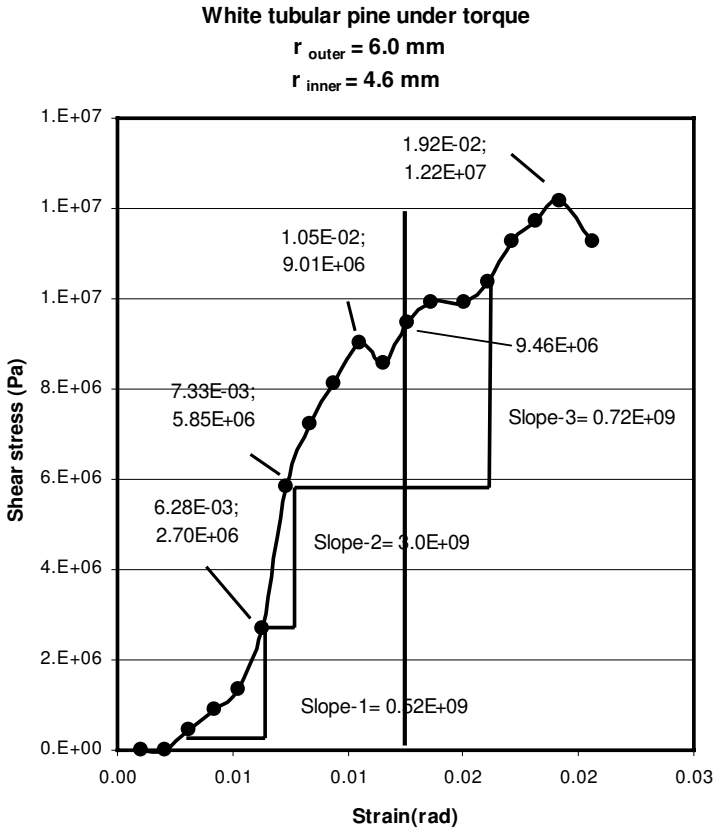

Figure 12. Curve for tubular white pine specimen and three-slope representation under forward torsional loading.

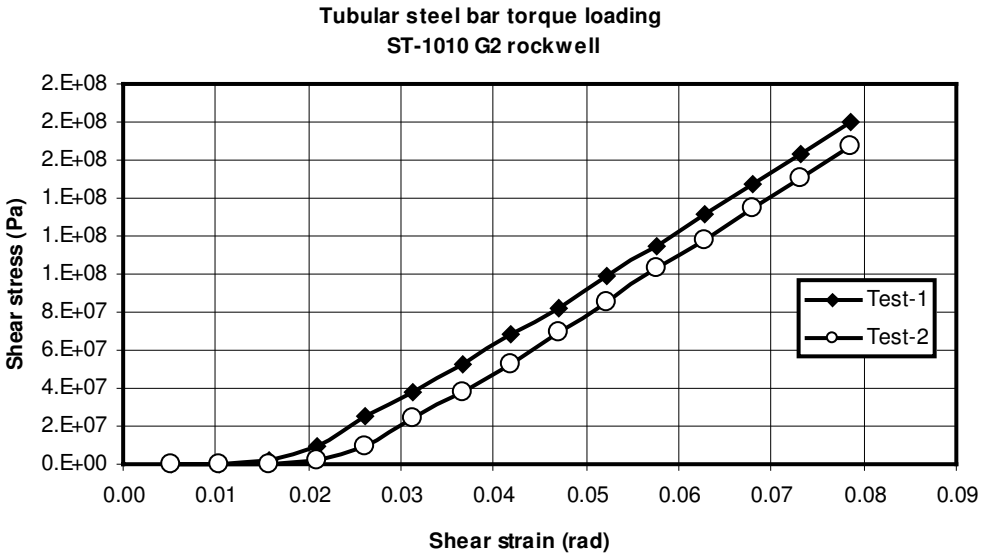

Figure 13. Curves for tubular steel specimens under torsion loading.

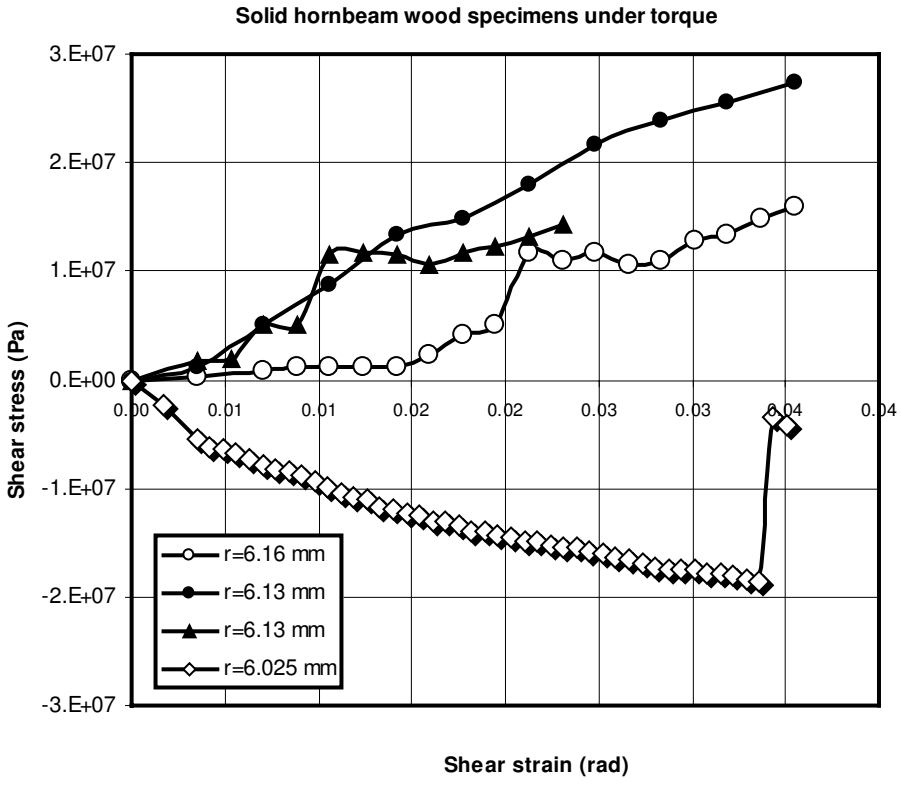

Figure 14. Hornbeam solid specimens under 3 different forward and 1 backward torsion loading.

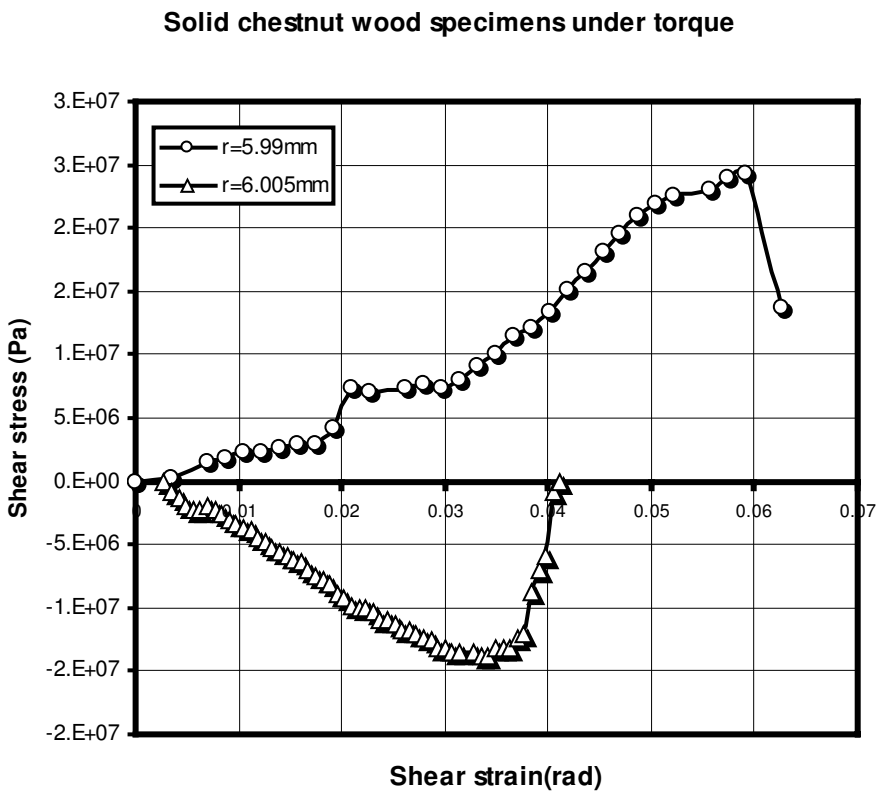

Figure 15. Chestnut solid specimens under 1 forward and 1 backward torsion loading.

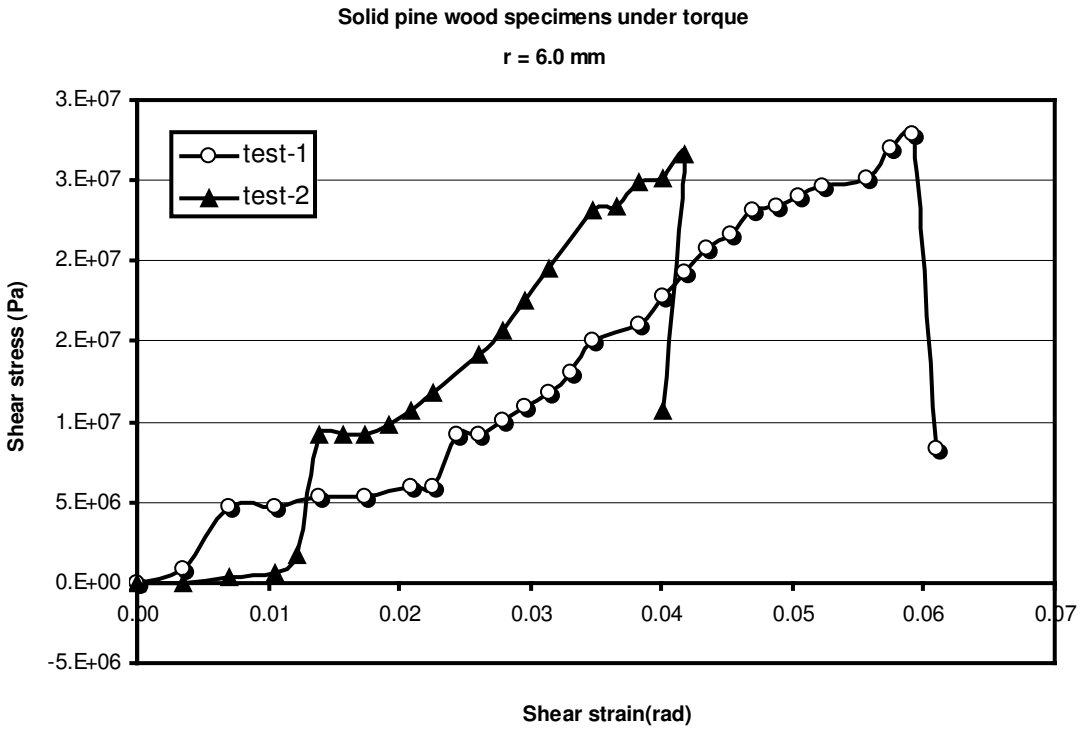

Figure 16. Pine solid specimens under forward torsion loading.

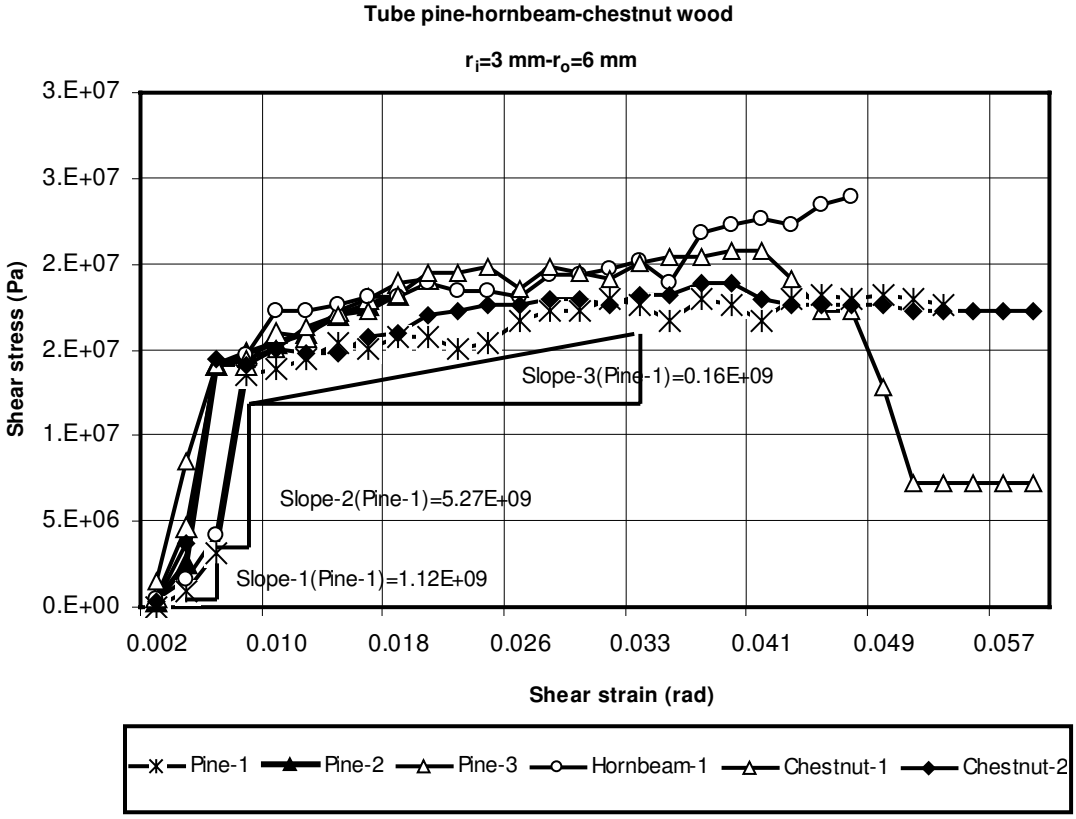

Figure 17. Curves for tubular pine, hornbeam and chestnut specimens and three-slope representation of specimen (Pine-1) under forward loading.

From all of the shear stress-strain curves for wood under torsional loading we observe segments of slightly parabolic curves with different slopes. In general, 3 slightly linear regions of the shear stress-strain curve can be distinguished. Sample representations are presented in Figures 12 and 17. Three slopes are shown in these graphs with their values. The second region always has a sharp stress increment with a few data points while the first and third regions have relatively small inclinations that include considerably large amount of data. The shear modulus G_{12} values are calculated and tabulated from the second region. The results of the torsional tests carried out on various wood species are also given in Tables 3-6 and the related statistical data are tabulated in Table 7 in detail. As seen from Table 7, quite large values of coefficients of variation (c.v.) were obtained. This variation may be affected to some extent by the data taken from the second linear elastic region, which have a sharp stress increment as mentioned above, rather than considering an average value of the entire response having less variation. Although there is less variation in the first and third linear regions, the calculations were not based on these regions because the complete grasp of the specimen occurred during the development of the first region and in the third region in general the elastic limit was exceeded. In an experimental investigation, Bektaş et al. (2002) carried out compression, static bending, impact bending, and shear strength tests on prismatic beech wood specimens in which the coefficient of variation was as high as 35%. All the shear tests were carried out parallel to the grains. However, in the torsion tests performed on round specimens in the present study it was not possible to measure shear strength perfectly parallel to grains. The structural complexity of wood depends mainly on the unidirectional grain angles through the thickness of the specimens. The specimens used have variable grain angles θ, which are measured with respect to the twist axis within the range 0° to $+35^\circ$. As expected, the variable grain angles affect significantly the stress-strain distributions under torsional loadings. Furthermore, during the preparation of the

round specimens the occurrence of undetected cracks or defects at the inner or outer surfaces could cause the stress concentration at those points. This problem does not exist in pure shear tests since the average shear stress calculations are based on an internal plane area that is not affected by stress concentrations to the same extent. It should also be noted that although the moisture contents were the same the specimens were extracted from different portions of different trees of the same wood species. This constitutes another factor affecting the large variations in the test results.

From the results obtained, it is also found that the torsional response of wood depends on the geometry (solid or tubular specimens) and on the application direction of the torque relative to the fiber directions as well. It can also noted that, when the Young's modulus E_{11} (Günay and Sönmez, 2003) and the shear modulus G_{12} for wood are compared, Young's modulus is found to be approximately 10 times larger than the shear modulus.

Hysteresis tests of solid and tubular specimens

The hysteresis curves are obtained for the nonlinear permanent deformation analysis under torsional loading with unloading and reloading steps. To the best of our knowledge, there are few published data presenting the hysteresis behavior of solid and tubular wooden bars under torsional loading.

In Figure 18 the results for a hornbeam solid specimen under 2 cyclic forward and backward loading show clearly the permanent deformations occurring in the wood specimens. Except for the initial forward loading, there are no differences in the slopes of the shear stress-strain curves. This shows that no additional strain energy is lost during the repeated hysteresis cycles within the tested $\tau - \gamma$ ranges. Figures 19 represents one forward and one backward cyclic loading of the solid hornbeam specimen. The shear stress and shear strain values reached $\tau = 25.6$ MPa and $\gamma = 0.036$ rad in forward loading, which caused a sudden drop in the shear stress value without resulting in an open crack. The specimen was then unloaded completely and the loading was reversed, decreasing the stress to $\tau = -21$ MPa with $\gamma = -0.080$ rad where the gross failure of the specimen occurred.

In Figure 20, the pine specimen was loaded until the shear stress reached approximately 30 MPa. The unloading process after this stress level caused permanent shear strain remaining in the wood specimen. Application of 2-cycles causes additional strain energy lost during the repeated hysteresis cycles within the variable $\tau - \gamma$ ranges.

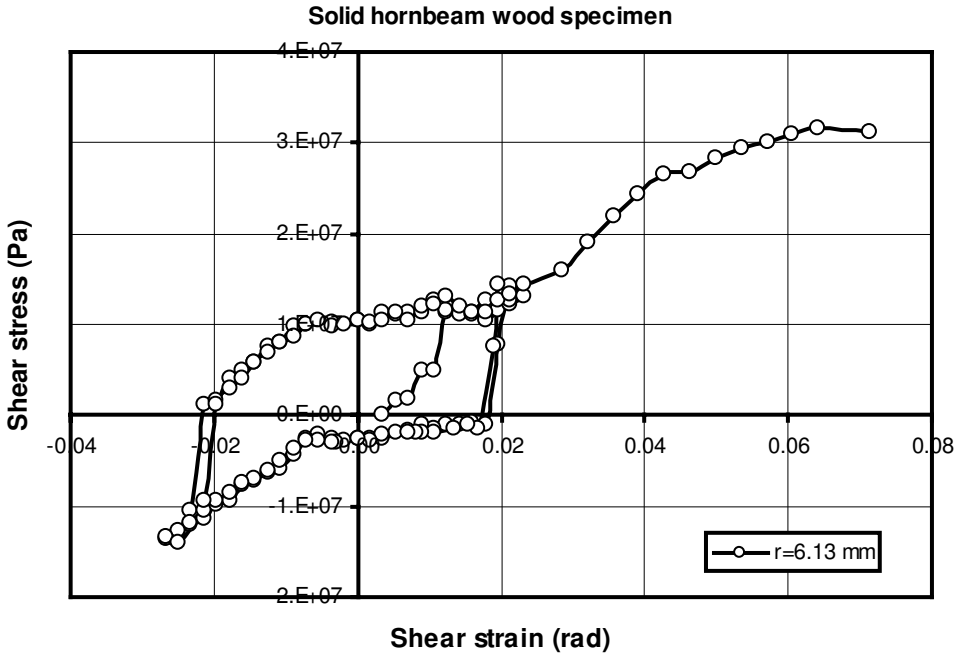

Figure 18. Hornbeam solid specimen under 2-cycle forward/backward loading.

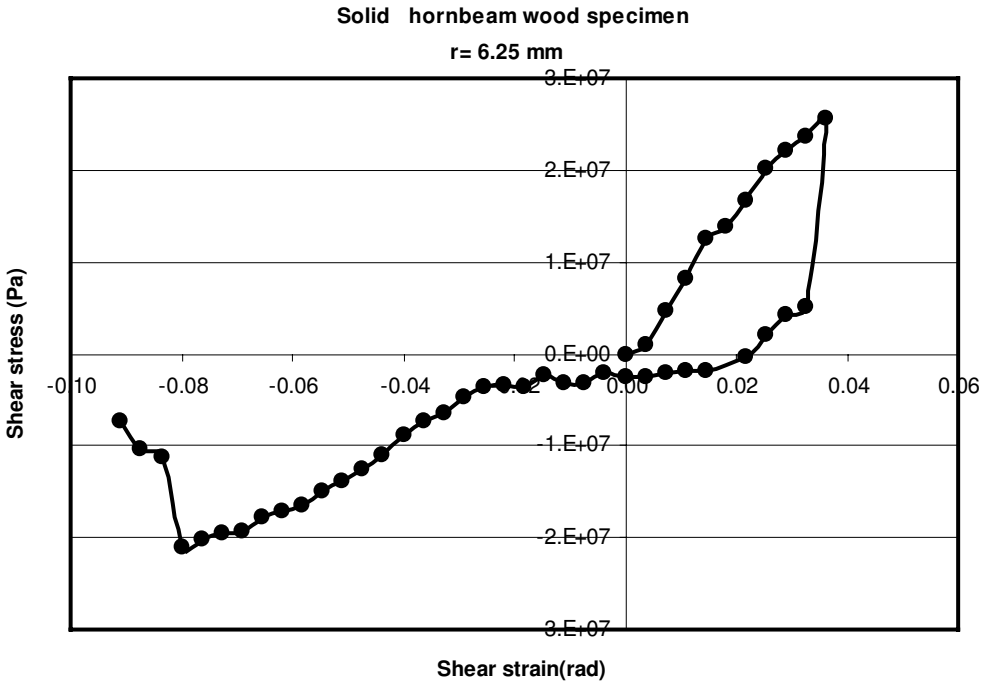

Figure 19. Hornbeam solid specimen under 1-cycle forward/backward torsion loading.

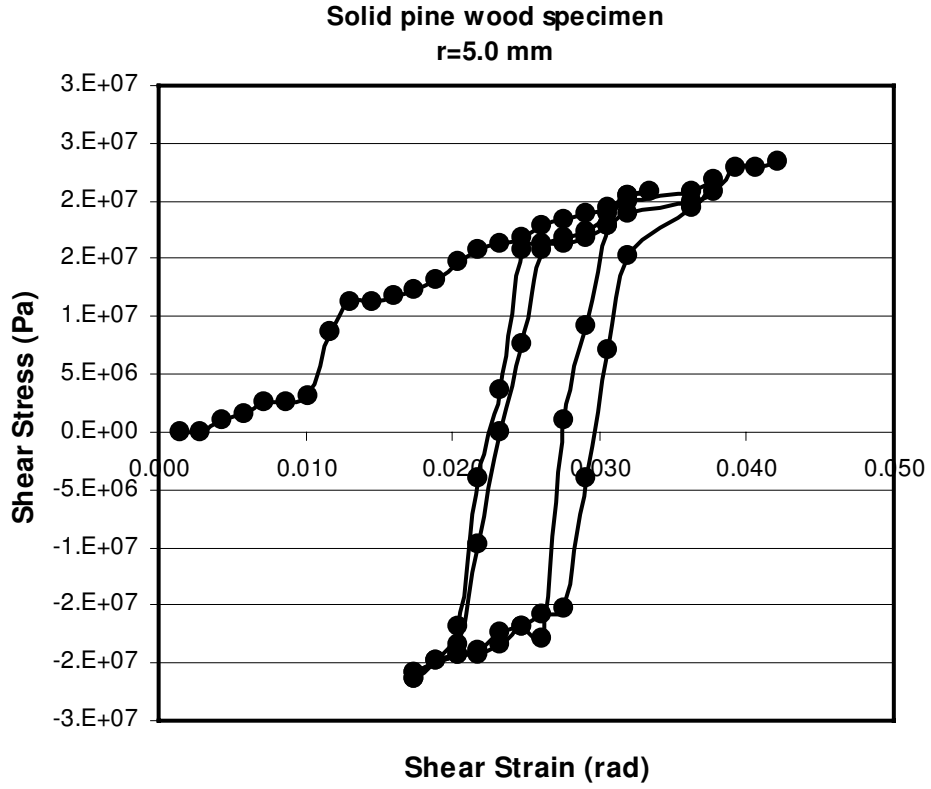

Figure 20. Pine solid specimen under 2-cycle forward / backward loading.

Figure 21 represents the solid beech specimen under 9 cyclic loading and unloading steps. A series of forward loading and unloading paths follow almost linear stress-strain curves. It is noted that there is no reduction in the stress level in the hysteresis behavior. The peak of each loading cycle reaches the same stress value and follows its characteristic linear path when the loading is further increased.

In Figure 22 cyclic loading and unloading steps were carried out on pine specimens. For 3 loading steps, the shear stress was increased up to $\approx$ 13 MPa,and then the specimens were subjected to reversed loading until zero shear strain was reached. It is noted that no permanent deformation remained in the specimen after the first 3 unloading cycles because of the low shear stress level in each case. The first 3 curves show small amounts of strain energy lost during the repeated forward/backward cycles within $\tau - \gamma$ ranges. The curves become parabolic during the third cycle. After this step, backward and forward loading steps follow linear paths.

Figure 23 represents one reverse cyclic and one forward loading of tubular pine specimen. Both responses are slightly parabolic and there is a significant difference in the slopes of stress-strain curves for reverse loading/unloading and forward loading.

Figures 24-26 show the hysteresis loops of the solid beech specimen for 3 different test specimen radii: $r = 3.25$ mm, $r = 5$ mm, $r = 6.25$ mm. Since unloading is done from a sufficiently high stress value, permanent strain remained in the test specimens upon complete unloading. It is interesting to note that, in each experiment, the stress level reaches the same stress value or its characteristic curve path at the end of the hysteresis loop.

Shear stress relaxation tests of solid specimens

Stress relaxation is defined as the behavior of stress reaching a peak and then decreasing or relaxing over a time under a fixed level of shear strain in a static torsion test. The specimens are loaded to a certain torque load below the fracture load and the angle of twist is held at a fixed position. The relaxation of the torque within the time scale is recorded for a long period, and the results are plotted for hornbeam, beech, and pine specimens in Figure 27. Hornbeam specimen had been relaxed from 7.2 to 23 N.m. in the first hour. For the beech specimen, which has the same geometrical values as the pine, the torque decreased from 7.75 to 2.3 N.m. within 11,000 min. The torque in the pine specimen decreased exponentially from 3.4 to 1.9 N.m within 10,000 min. It is noted that beech and hornbeam are relaxing 2 times faster than pine. The torque relaxation curves indicate that, for all wood species, the shear stress decays exponentially with time. Therefore, wood can be considered a viscoelastic material that obeys the Maxwell model of stress relaxation. According to this model, the stress relaxes completely as time goes to infinity.

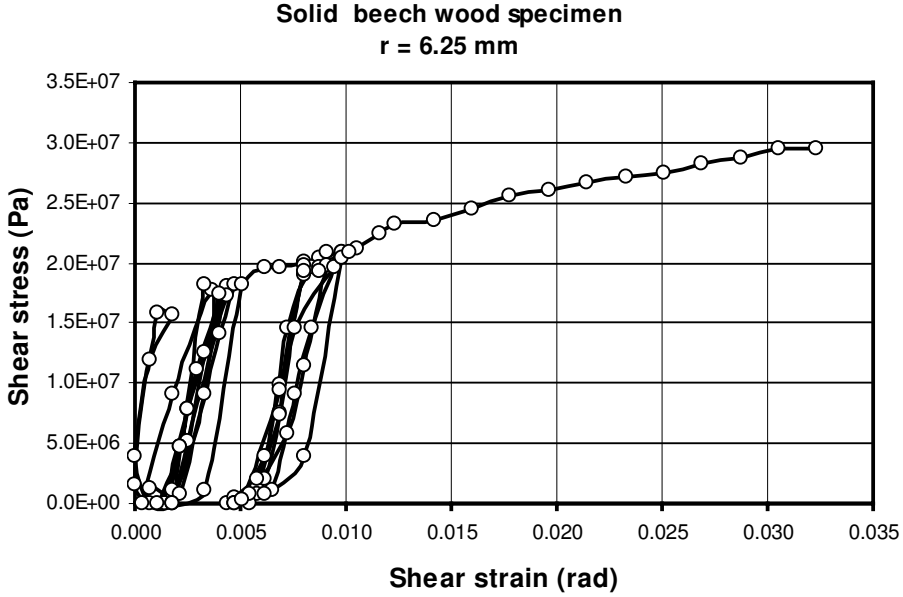

Figure 21. Beech solid specimen under 9-cycle forward loading.

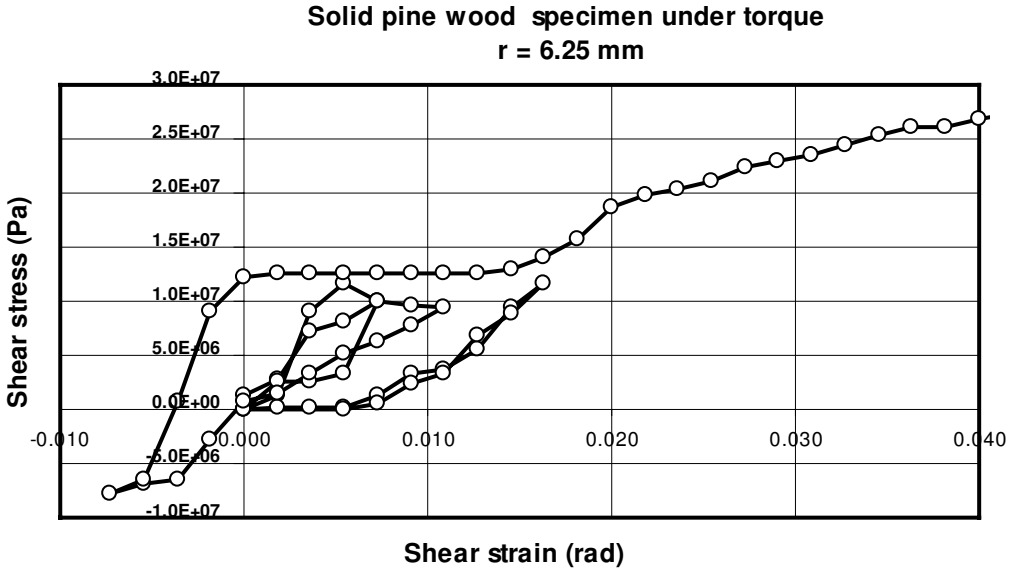

Figure 22. Pine solid specimen under 3-cycle forward 1-cycle backward loading.

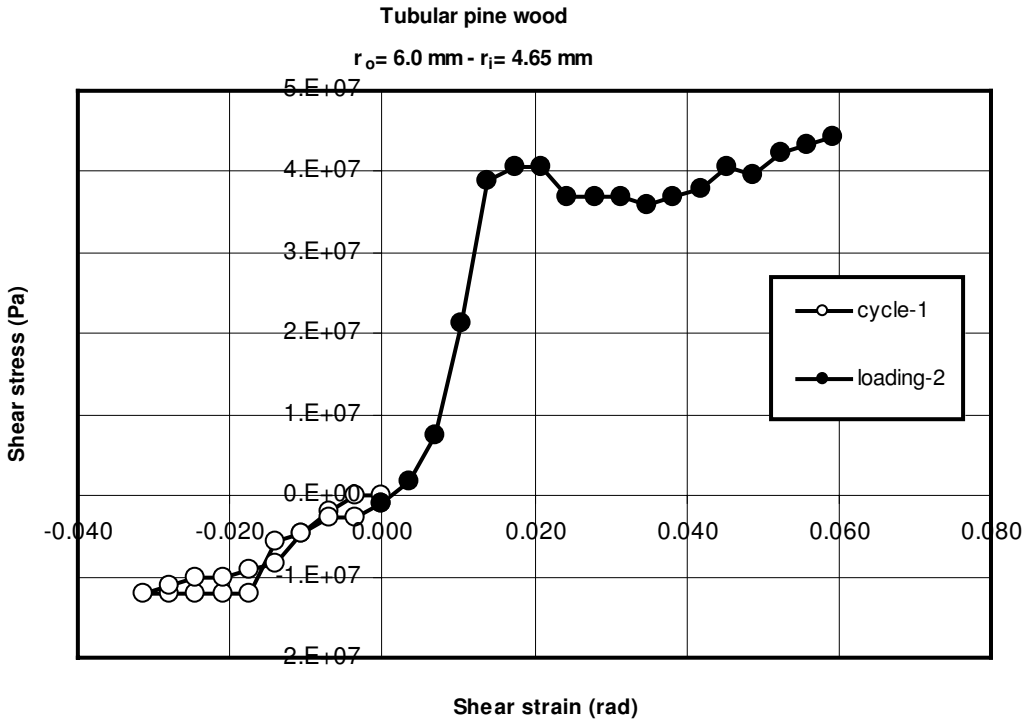

Figure 23. Pine specimen under 1-cycle backward and then continuous forward loading.

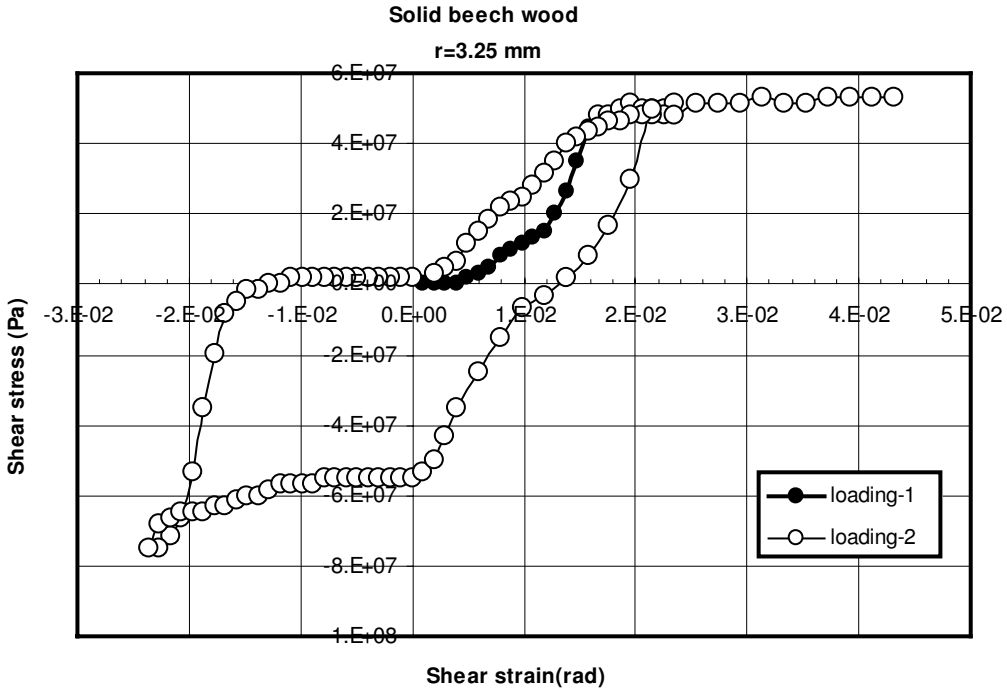

Figure 24. Curves for solid beech under 1 forward loading and 1 complete cycle.

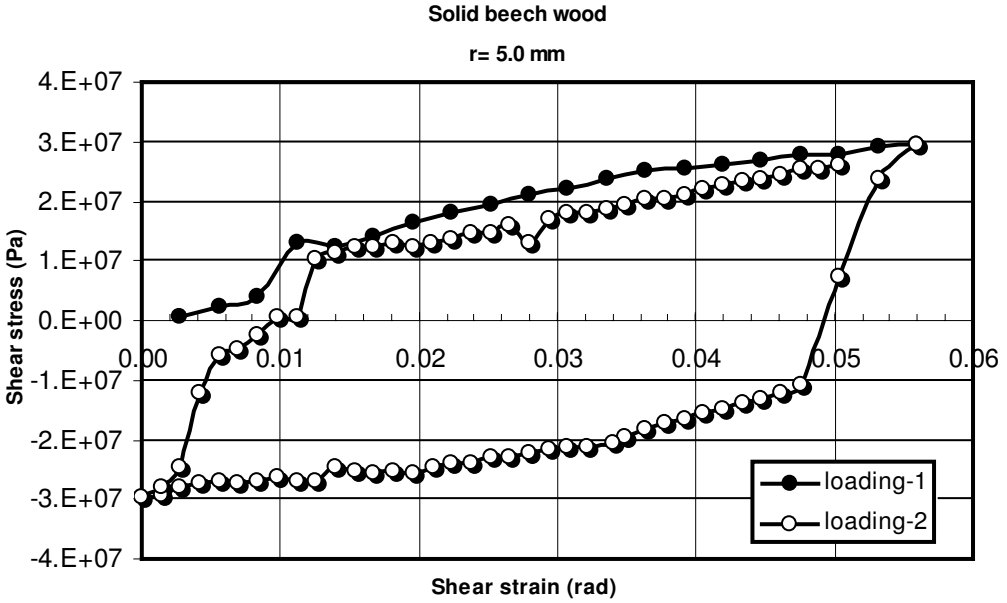

Figure 25. Curves for solid beech under 1 forward loading and 1 complete cycle.

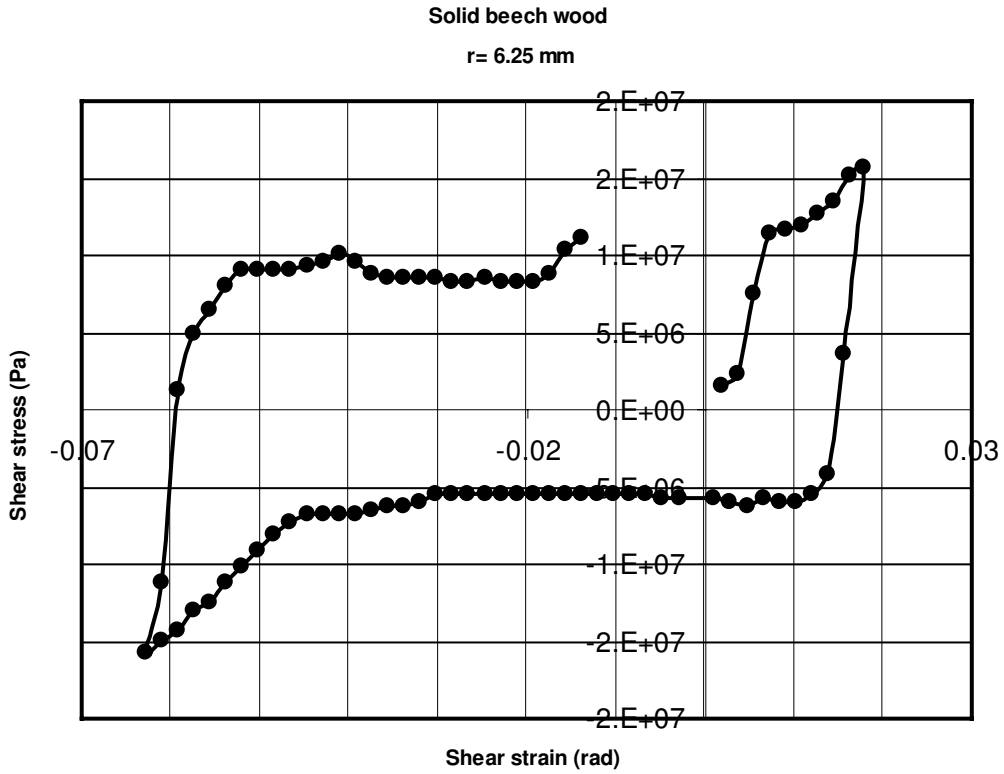

Figure 26. Curves for solid beech wood under 1 forward loading and 1 complete cycle.

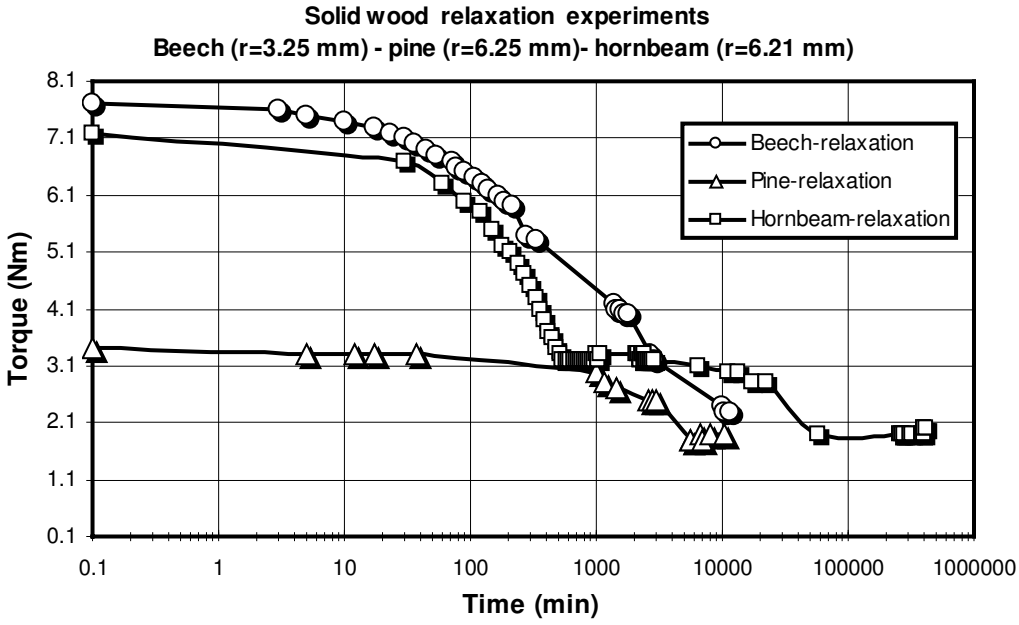

Figure 27. Stress relaxation curves of the beech, pine and hornbeam solid specimens.

Conclusions

Wood is a good example of an orthotropic fiber composite material with its organic structure. Because of the complexity in the cellulosic structure at micro level, the general mechanical behavior is not known clearly. Furthermore, the behavior of wood material changes with the type of loading, temperature, moisture content, grain angles, material density, the growth condition, and the age of the tree from which the specimen is taken.

From the results of the torsion tests performed in the present study, the following conclusions can be drawn:

1. In general, the response of wood to torsional loading exhibits a flexible character that is affected by specific alignments of the grains and type. The presence of possible defects in micro levels produced during the preparation of the specimens is also important.

2. Failures occurred due to a longitudinal crack that propagated along the grain directions. If the grain angles are parallel to the longitudinal axis the crack propagates along the twist axis more slowly since the ends of the test specimen act as a sort of reinforcement against axial crack propagation. Therefore, for 0^o grain angles, the failures of the specimens are incomplete.

3. Failure characteristics of the test specimens in static loading depend on the sense of the applied torque, and the type and geometry of the wood species.

4. In cyclic torsional loading, if the amplitude of the applied torque is within the elastic range, the specimens are resistant to alternating loads without having any residual distortion. However, if a specimen is loaded beyond the proportional limit, a hysteresis loop is observed, which repeats itself in successive cycles. In samples with 0^ograin angles, the hysteresis loops exhibit similar stress-strain gradients in forward and backward loading. Shear and normal stresses are distributed equally throughout the fiber and matrix combination.

5. Pine is more flexible compared to chestnut, hornbeam, and beech. It can undergo larger twist angles before the nucleation of any cracks.

6. Tubular specimens exhibit a sudden rise in stress-strain curves before transition to a permanent deformation zone.

7. In general, shear stress-strain curves consist of 3 slightly linear portions with different slopes. The second region has the steepest slope, while the third region is much wider than the others and corresponds to permanent deformation zone of the specimens.

8. Displacement controlled relaxation static tests of wood species show that wood is a viscoelastic material that obeys the Maxwell model during relaxation.

Based on the various experiments performed in the present study, it is concluded that much experimental and theoretical investigation remains to be done to understand the mechanical behavior of wood in torsion.

Acknowledgments

All the experiments were performed at the Mechanics Laboratory of Gazi University Mechanical Engineering Department. The authors would like to acknowledge the help of Asst. Prof. Dr. Rahmi Aras and G.U. Graduation Project course students for supplying the wood material, and technician Kadir Yılmaz for the preparation of solid and thin tubular wood specimens in this research.

Nomenclature

A	grip dimension (mm)
a, b	Iosipescu shear test fixture constants
c.v.	coefficient of variation
D_i, D_o	inner and outer diameters (m)
E_1, E_2, E_3, G_{12}, G_{23}, G_{13}	Young's and shear moduli of the orthotropic material in principal directions $\left(N/m^2\right)$
E_x, E_y, E_z, G_{xy}, G_{xz}, G_{yz}	Young's and shear moduli of the orthotropic material through x, y, z axes of the cartesian coordinate system $\left(N/m^2\right)$
J	polar moment of inertia $\left(m^4\right)$
H	grip dimension (mm)

k	constant number (Lekhnitskii) which is obtained from series expansion
k_{zx}, k_{yz}	instantaneous shear modulus values
L_g, L	gauge and total length of specimen (mm)
r_i, r_o	inner and outer radii (m)
st.d.	standard deviation
T	torque (N.m)

Greek symbols

ε_x, ε_y, ε_z	normal strain components of the orthotropic material (rad)
ϕ	angle of twist (rad)
$\gamma_{13}, \gamma_{23}, \gamma_{12}$	shear strain components of the orthotropic material in principal directions (rad)
η_{xs}	Lekhnitskii elastic constant
ν_{xy}, ν_{xz}, ν_{yz}	Poisson's ratios of the orthotropic material
θ	grain angle measured from the twist axis (degree)
σ_x, σ_y, σ_z	normal stress components of the orthotropic material $\left(N/m^2\right)$
σ_1, σ_2, σ_3	normal stress components of the orthotropic material in principal directions $\left(N/m^2\right)$
σ_t, σ_c, σ_{ut}, σ_{uc}	elastic tensile, compressive, ultimate tensile and ultimate compressive stress $\left(N/m^2\right)$
τ_{13}, τ_{23}, τ_{12}	shear stress components of the orthotropic material $\left(N/m^2\right)$
τ_s, γ_s	average shear stress and strain$\left(N/m^2\right)$,(rad)

References

ASTM Standard Methods for Testing Small Clear Specimens of Timber., ASTM Stand., 143-152, 1972.

Beall, F.C., "Fundamentals of Acoustic Emission and Acousto-Ultrasonics". Proceedings of the 6th Nondestructive Testing of Wood Symposium. Washington State University Pullman, WA., USA, 3-28, 1987.

Bektaş, İ., Güler, C. and Baştürk, M.A., "Experimental Investigation of the Mechanical Behavior of Solid and Tubular Wood Species under Torsional Loadings", Turk. J. Agric. For., 26, 147-154, 2002.

Bodig, J. and Jayne, B.A., In: Mechanics of Wood and Wood Composites, p 158, Van Nostrand Reinhold Company Inc., New York, USA, 1982.

Bodig, J., "The Process of NDE Research for Wood and Wood Composites", 12th International Symposium on Nondestructive Testing of Wood, www.ndt.net/article/v06n03/bodig/bodig.htm, NDT.net, 6, 2001.

BSI, Methods of Testing Small Clear Specimens of Timber, British Stand., 373, 1957.

Bucur, V., "Elastic Symmetry for Wood Mechanical Characterization". WCU, 7-10, (www.sfa.asso.fr), 2003.

Bucur, V., Lanceleur P. and Roge B., "Acoustic Properties of Wood in Tridimensional Representation of Slowness Surfaces". Ultrasonics, 40, 537-541, 2002.

Bucur, V. and Rasolofosaon P.N.J., "Dynamic Elastic Anisotropy and Nonlinearity in Wood and Rock", Ultrasonics, 36, 813-824, 1998.

Bucur, V., "Techniques for High Resolution Imaging of Wood Structure—A Review", Measurement Science and Technology, 14, 91-98, 2003.

Chen, Z., Gabbitas, B. and Hunt, D., "The Fracture of Wood under Torsional Loading", J. Mater. Sci., 41, 7247-7259, 2006.

Çilesiz, U., "Torsion Test and Torsional Elasticity for Deformation of Nonhomogeneous Bars", G.U. Mechanical Engineering Department, Graduation Project, 2004.

Chandrupatla, T.R. and Belegundu, A.D., Introduction to Finite Elements in Engineering. 2nd Ed., Prentice Hall, New Jersey, 1997.

Dinus, R.J. and Welt T., "Tailoring Fiber Properties to Paper Manufacture—Recent Developments", TAPPI J, 127-139, 1997.

Forest Products Laboratory Wood Handbook, Gen Tech Rep(FPL-GTR-113). US Department of Agriculture Forest Serv. Madison WI, 463, 1999.

Govic, C.L.E. and Khebibeche, M., "Methodological Developments in the Testing of Wood Based Panels: Part I. Tensile and Compression Tests", Materials and Structures, 27, 229-236, 1994.

Groom, L., Mott, L. and Shaler, S., "Mechanical Properties of Individual Southern Pine Fibers: Part I. Determination and Variability of Stress-Strain Curves with Respect to Tree Height and Juvenility", Wood and Fiber Science, 34, 14-27, 2002.

Günay, E. and Sönmez, M., "Mechanical Behavior of Wood under Torsional and Tensile Loadings", G.U. Journal of Science, 16, 733-749, 2003.

Hayashi, K., Felix, B. and Govic, C.L.E., "Wood Viscoelastic Compliance Determination with Special Attention to Measurement Problems", Materials and Structures, 26, 370-376, 1993.

Hibbeler, R.C., Mechanics of Materials, Prentice Hall, New York, 1991.

Kazancılar, M. "İçi Dolu ve Tüp Şeklindeki Metal ve Ağaç Çubuklarda Burulma Deneyi", G.U. Mechanical Engineering Department, Graduation Project (in Turkish), 2004.

Kollmann F. and Coté, W.A., In: Principles of Wood Science and Technology I: Solid Wood. Springer-Verlag. Heidelberg, Germany, 1968.

Ifju, P.G., "The Shear Gauge for Reliable Shear Modulus Measurements of Composite Materials", Exp. Mech., 34, 369-378, 1994.

Lekhnitski, S.G., Theory of an Anisotropic Elastic Body. Holden-Day, San Francisco CA, 197-205, 1963.

Liu, J.Y., Flash, D., Ross, R.J. and Lichtenberg, G.J., "An Improved Shear Test Fixture Using the Iosipescu Specimen", ASME Mech Cellulosic Mater., 85, 139-147, 1999.

Liu, J.Y. and Ross, R.J., "Wood Mechanical Property Variation with Grain Slope", ASCE 12th Engineering Mechanics Conference, La Jolla, CA, 1351-1354, 1998.

Liu, J.Y., "Effects of Shear Coupling on Shear Properties of Wood", Wood and Fiber Science, 32, 458-465, 2000.

Mack, J.J., A Study of the Torsion Test, Progress, Report No.1: Effect of Size of Specimen. SUB Project TM 22/4. Commonwealth of Scientific and Industrial Research Organization Melbourne, Victoria, Australia, 1940.

Mack, J.J., Australian Methods for Mechanically Testing Small Clear Specimens of Timber, Commonwealth Scientific and Industrial Research Organization, Division of Building Research, Technical Paper (Second Series), Melbourne, 31, 1979.

Mal, A.K. and Cohen, Y.B., "Ultrasonic NDE of Bonded Solids", Proceedings of the International Workshop on Nondestructive Evolution for Performance of Civil Structures, University of Southern California, Los Angeles CA, USA, 299-308, 1988.

March, H.W., Kuenzi, H.W.E.W. and Kommers, W.J., Method of Measuring the Shearing Moduli in Wood, Report No.1301, USDA Forest Serv., Forest Prod Lab., Madison WI, 1942.

Örs Y., Çolakoglu G. and Çolak S., "Effect of Some Production Parameters on the Shear-Tensile Strength Bending Strength and Modulus of Elasticity of Poplar Plywood", J. Polytechnic, 4, 25-32, 2001.

Pagano, N.J. and Kim R.Y., "Interlaminar Shear Strength of Cloth-Reinforced Composites", Experimental Mechanics 28, 117-122, 1988.

Park, B.D. and Balatinecz, J.J., "Mechanical Properties of Wood-Fiber Toughened Isotactic Polypropylene Composites", Polymer Composites, 18, 79-89, 1997.

Pereira, J.L., Mechanical Behaviour of Wood Pinus Pinaster Ait in Traction on the Material Directions, MSc Thesis, University of Trás-os-Montes e Alto Douro, Vila Real, Portugal; In Portuguese, 2004.

Rammer, D.R. and McLean D.I., Recent Research on the Shear Strength of Wood Beams, Proceedings of the International Wood Engineering Conference, New Orleans LA, Louisiana State University, 2, 96-103, 1996.

Rezai, E. and Warner, R.R., "Polymer-Grafted Cellulose Fibers I. Enhanced Water Absorbency and Tensile Strength", Int. J. Appl. Polym. Sci., 65, 1463-1469, 1997.

Sarıkavak, Y., "Doğal Kompozit Olan Ağaç Malzemelerde Burulma Deneyi Düzeneğinin Kurulması ve Kayma Modüllerinin Tayini", G.U. Mechanical Engineering Department, Graduation Project (in Turkish), 2005.

TQ, TecQuipment SM21 Torsion Testing Machine Manual, Nottingham, UK, 1982.

Tsai, C.L. and Daniel I.M., "Determination of In-Plane and Out-of-Plane Shear Moduli of Composite Materials", Experimental Mechanics 30, 295-299, 1990.

Tsai, C.L., Daniel, I.M. and Yaniv G., "Torsional Response of Rectangular Composite Laminates", J. Appl. Mech., Trans ASME, 57, 383-387, 1990.

Winandy, J.E., Wood Properties, Arntzen Charles J Ed., Encyclopedia of Agricultural Science, Ch.4, Orlando FL, Academic Press, 1994.

Winandy, J.E. and Rowell, R.M., Handbook of Wood Chemistry and Wood Composites, Ch.11:, Chemistry of Wood Strength, www.fpl.fs.fed.us/documnts/pdf2005/fpl_2005_winandy004.pdf, CRC Press, Washington, D.C., 2005.

Woodward, C. and Minor, J., "Failure Theories for Douglas Fir in Tension", J. Struct. Eng., 114, 2808-2813, 1988.

Xavier, J.C, Garrido, N.M., Oliveria, M., Morais, J.L., Camanho, P.P. and Pierron, F., "A Comparison Between the Iosipescu and Off-Axis Shear Test Methods for the Characterization of Pinus Pinaster Ait", Composites Part A, 35, 827-840, 2004.

Yamasaki, M. and Sasaki, Y., "Effect of Loading Method on the Elastic Properties of Wood (Japanese Cypress) under Combined Axial Force and Torque", Transactions of the Japan Society of Mechanical Engineers, 66, 48-54, 2000.

Yamasaki, M. and Sasaki Y., "Failure Behaviour of Wood (Japanese Cypress) under Combined Axial Force and Torque", Transactions of the Japan Society of Mechanical Engineers, 66, 172-179, 2000.

Yoshihara, H., Ohsaki, H., Kubojima, Y. and Ohta, M., "Comparisons of Shear Stress/Strain Relations of Wood Obtained by Iosipescu and Torsion Tests", Wood and Fiber Science, 33, 275-283, 2001.

Yoshihara, H. and Ohta, M., "Measurement of the Shear Moduli of Wood by the Torsion of a Rectangular Bar", Mokuzai Gakkaishi, 39, 993-997, 2001.

Zahreddine, N. and Araar, M., "Applied Data for Modeling the Behavior in Cyclic Torsion of Beams in Glued-Laminated Wood: Influence of Amplitude", J. Wood Sci., 49, 36-41, 2003.

Zidi, M., "Finite Torsion and Shearing of a Compressible and Anisotropic Tube", Int. J. Nonlinear Mechanics, 35, 1115-1126, 2000.

Appendix

Plane stress state, strain-stress relations of an orthotropic material used in experimental studies.

$$\begin{bmatrix} \varepsilon_x \\ \varepsilon_y \\ \gamma_s \end{bmatrix} = \begin{bmatrix} 1/E_x & -\nu_{yx}/E_y & \eta_{sx}/G_{xy} \\ -\nu_{yx}/E_x & 1/E_y & \eta_{sy}/G_{xy} \\ \eta_{xs}/E_x & \eta_{ys}/E_y & 1/G_{xy} \end{bmatrix} \begin{bmatrix} \sigma_x \\ \sigma_y \\ \tau_s \end{bmatrix} \tag{A1}$$

Lekhnitskii (1963) and Yoshihara et al. (2001) gave the shear modulus formulations of orthotropic material with the following series expansions:

$$G_{zx} = \frac{k_{zx}}{a^2\, b\, k} \left[-\frac{8}{\pi^2} \sqrt{\frac{G_{zx}}{G_{yz}}} \sum_{j=1}^{\infty} \frac{(-1)^{j-1}}{(2j-1)^2} \tanh \frac{(2j-1)\ \pi\, b}{2a} \sqrt{\frac{G_{zx}}{G_{yz}}} \right] \tag{A2}$$

$$G_{yz} = \frac{k_{yz}}{a^2\, b\, k} \left[1 - 2 \left(\frac{2}{\pi}\right)^2 \sum_{j=1}^{\infty} \frac{1}{(2j-1)^2} \left\{ \cosh \frac{(2j-1)\ \pi\, b}{2a} \sqrt{\frac{G_{zx}}{G_{yz}}} \right\}^{-1} \right] \tag{A3}$$

Here k_{zx} , k_{yz} are initially assumed slopes of the torsional moment-shear strain curve or the instantaneous shear modulus values. The geometric constants are: $a = 22\ mm$, $b = 12\, mm$ defined on the Iosipescu shear test fixture. k is calculated by series expansion as (Lekhnitskii, 1963);

$$k = \frac{1}{3} - \frac{2\ a}{b} \sqrt{\frac{G_{yz}}{G_{zx}}} \left(\frac{2}{\pi}\right)^5 \sum_{j=1}^{\infty} \frac{1}{(2j-1)^5} \tanh \frac{(2j-1)\ \pi\, b}{2\ a} \sqrt{\frac{G_{zx}}{G_{yz}}} \tag{A4}$$

Transversely isotropic elastic materials have 5 independent elastic constants and strain-stress relation can be expressed in the following form in combined loading:

$$\begin{bmatrix} \varepsilon_{1} \\ \varepsilon_{2} \\ \varepsilon_{3} \\ \gamma_{23} \\ \gamma_{31} \\ \gamma_{12} \end{bmatrix} = \begin{bmatrix} \frac{1}{E_1} & -\frac{\nu_{21}}{E_2} & -\frac{\nu_{31}}{E_3} & 0 & 0 & 0 \\ -\frac{\nu_{12}}{E_1} & \frac{1}{E_2} & -\frac{\nu_{32}}{E_3} & 0 & 0 & 0 \\ -\frac{\nu_{13}}{E_1} & -\frac{\nu_{23}}{E_2} & \frac{1}{E_3} & 0 & 0 & 0 \\ 0 & 0 & 0 & \frac{1}{G_{23}} & 0 & 0 \\ 0 & 0 & 0 & 0 & \frac{1}{G_{31}} & 0 \\ 0 & 0 & 0 & 0 & 0 & 2\left(\frac{1}{E_1}+\frac{\nu_{21}}{E_2}\right) \end{bmatrix} \begin{bmatrix} \sigma_{1} \\ \sigma_{2} \\ \sigma_{3} \\ \tau_{23} \\ \tau_{31} \\ \tau_{12} \end{bmatrix} \tag{A5}$$